Study of Internal Structure of a Neutron Star with Quark Matter

Tasha Gautam
MP15005

A dissertation submitted for the partial fulfilment
of MS degree in Science

Under the guidence of
Dr. Satyajit Jena

April 2018

Indian Institute of Science Education and Research Mohali
Sector - 81, SAS Nagar, Mohali 140306, Punjab, India

Certificate of Examination

This is to certify that the dissertation titled **"Study of Internal Structure of a Neutron Star with Quark Matter"** submitted by **Tasha Gautam** (Reg. No. MP15005) for the partial fulfillment of MS dual degree programme of the Institute, has been examined by the thesis committee duly appointed by the Institute. The committee finds the work done by the candidate satisfactory and recommends that the report be accepted.

Dr. Kinjalk Lochan Dr. H.K. Jassal Dr. Satyajit Jena
(Supervisor)

Dated: 20.04.2018

Declaration

The work presented in this dissertation has been carried out by me under the guidance of Dr. Satyajit Jena at the Indian Institute of Science Education and Research Mohali.

This work has not been submitted in part or in full for a degree, a diploma, or a fellowship to any other university or institute. Whenever contributions of others are involved, every effort is made to indicate this clearly, with due acknowledgement of collaborative research and discussions. This thesis is a bonafide record of original work done by me and all sources listed within have been detailed in the bibliography.

Tasha Gautam
(Candidate)

Dated: April 20, 2018

In my capacity as the supervisor of the candidate's project work, I certify that the above statements by the candidate are true to the best of my knowledge.

Dr. Satyajit Jena
(Supervisor)

Acknowledgement

First and foremost I praise and thank the almighty for being the unfailing source of support, comfort and strength throughout the completion of my project work.

I would like to thank Director Prof. Debi Prasad Sarkar, Indian Institute of Science Education and Research Mohali and Prof. Jasjeet Singh Bagla, Head of Department of Physical Science, for the infrastructure, library facilities, research facilities and for exposing myself to the working environment of a full–fledged research institute.

It's an honour and proud privilege in expressing my deepest and sincere gratitude to Dr. Satyajit Jena, Assistant Professor, Department of Physical sciences, Indian Institute of Science Education and Research Mohali, for his kindness and support, for accepting my request to work under his guidance and for enabling me in the pursuit of my career.

I express my warm appreciation and most respectful regards to Dr. Kinjalk Lochan and Dr. H. K. Jassal, my thesis committee members for their valuable suggestions and comments during the committee meetings.

I am so obliged and extremely thankful to Dr. Kinjalk Lochan, for patiently teaching me everything from basics. He helped me throughout this project by providing me with necessary intellectual input in most needful times. Without his help and effort, this project work would be incomplete.

I would like to thank my lab members, Shahina Ali, Anjaly S. Menon, Nishat Fiza, Akhil Bharadwaj, Asish Moharana, Shubham Varma, Neeraj Maan and Kartik Joshi for making the lab lively and lending a hand at times when I needed.

I express my enormous love and affection to my family members, for their unconditional love and support which I always received. Finally, I would like to express my love and care to my friends Tania Sharma, Gaurav Saxena and my classmates for their unselfish, loyal, true benevolent concern for me.

Tasha Gautam
MP15005
IISER Mohali

Contents

List of Figures

Abstract

Neutron stars are the dense core of matter left after the supernova explosions of massive stars, they comprise of the most densest form of matter with densities going upto nearly 2-10 times the nuclear saturation density. Correct prediction of macroscopic properties such as mass and radius of neutron stars is necessary to study the extreme states of matter found inside the structure of neutron star as well as to study the implications of such scenarios on the metric of space time. There have been many uncertainties on the measurement of neutron star's radius as well as on determining the maximum mass limit of neutron stars. This uncertainty is mainly due to the limited knowledge of the equation of state(EOS) of the matter present inside neutron star. The largely varying densities inside neutron star results in significantly different states of matter inside, varying from Iron like densities at the surface to possibly exotic state with immense densities of nearly $10^{15} gcm^3$ at the core. This work involves the study of several theoretical models (such as BPS model, polytropic approaches, etc.) for the lesser dense hadronic part of neutron star. A C++ code for solving the structural equations (TOV equations) considering the general relativistic correction has been developed. I have used many models of EOS to evaluate the mass-radius relationship. Further, due to the immense densities inside a neutron star, there is a possibility of the existence of pure-quark matter in "De-confined" state. The resulting consequence of such state would be to reduce the volume of the star. The effect of such state and the resulting changes in the radii have been discussed and calculated in this thesis.

Chapter 1

Introduction

Neutron Stars are one of the most densest forms of massive objects in the universe. With extreme densities and relatively low temperatures, the matter found inside them cannot be produced by the laboratories on earth, this makes them the only possible laboratories to test the theories of dense matter physics and provide connections between nuclear physics, particle physics, and astrophysics. The formation mechanism of such dense cores of matter is through the supernovae explosion during the death of a massive star.

A main-sequence star uses its hydrogen as a fuel to burn in Helium and higher atomic mass elements. The energy generated from fusion reactions is required to sustain its thermodynamic equilibrium. A neutron star is formed when a massive star (mass ranges about $8 - 10M_0$) runs out of its fuel and is unable to sustain the gravitational force, hence undergoing a supernova explosion. The densities in such objects are significantly varying from iron-like densities to several times the nuclear saturation density of nuclei. But considering the immense densities, the temperatures (at around 10^6 K) near the core of neutron stars are comparably less, and the matter is hence effectively cold inside the neutron stars. This peculiar property makes them the only possible laboratories to study 'dense' and 'cold' matter. At extreme densities, the baryonic matter itself melts into its constituent particles, the nuclei present inside becomes more and more neutron-rich, and the neutrons, protons, and electrons form a Fermi-sea of free particles. The structure at further densities ($2 - 7$ times nuclear saturation density) is so dense that mesons such as Kaons begin to form degenerate condensates (refer to section 1.3) and result into the formation of exotic stars.

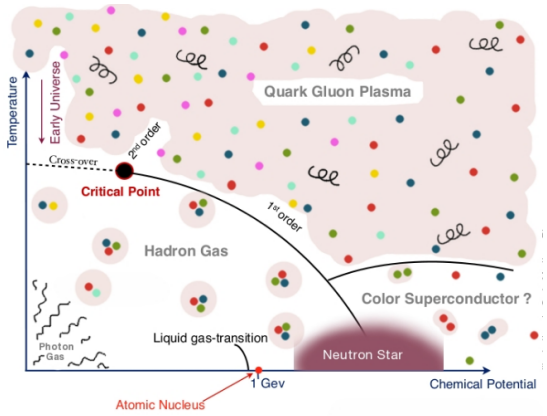

Figure 1.1: Plot of Temperature with chemical potential shows the phase transition to QGP at high chemical potential

The macroscopic properties of a neutron star such as its mass and radius give a direct indication of the state of matter which can be found inside. The estimation of masses can be made with certain uncertainties through the observations of binary systems of neutron stars. But the estimation of the radius is highly uncertain. It is due to this uncertainty in the correct prediction of masses and radii as well as the small sample of neutron stars observed that the states of matter cannot be predicted with acceptable certainties. Also, the parameters predicted from the accelerators allow for large flexibility further making the prediction for the state more uncertain.

Further, at high temperature or chemical potential, the matter is in the form of Quark-Gluon Plasma (QGP) in which the fundamental degrees of freedom are quarks and gluons. Such phase transition can occur due to the immense chemical potential or mass densities (see fig. 1.1) and hence there exist the possibility of the existence of quark matter state at the core of massive neutron stars. Such state has a peculiar property of "De-confinement", in which the quarks behave as asymptotically free particles with smaller overall volume. This state if present inside a neutron star would result in a smaller radius of the neutron star. These implications have been speculated in this thesis, and the resulting changes in the radii are predicted if quark matter is present inside the core.

This work also takes a closer look at the internal structure of a neutron star and considers various possibilities of different states of matter which can exist at varying densities. The effect of such states on the macroscopic properties has been discussed. The interpolation

methods to fit two different states while maintaining the physical validity are also discussed. Finally, mass and radius relationships have been developed and compared with the observations obtained so far.

The states of matter present inside a neutron star are largely dependent upon the process which results in its formation. Hence, to have a better picture of the matter inside it, it is important to study the formation mechanism discussed in next section in detail.

1.1 Birth of a Neutron Star

In a main sequence star the most prominent reaction is the burning of Hydrogen to produce Helium as given by the 3 step p-p chain reaction:

$$^1H +^1 H \rightarrow^2 H + e^+ + \nu_e \tag{1.1}$$

$$^2H +^1 H \rightarrow^3 He + \gamma \tag{1.2}$$

$$^3He +^3 He \rightarrow^4 He +^1 H +^1 H \tag{1.3}$$

The process of energy generation from this fusion process (about 25 MeV) is able to support the star against its contracting force of gravity, resulting in the Hydro-static equilibrium. When most of the hydrogen is burnt into helium, the helium atom starts to fuse into each other to produce heavier carbon atoms. This process occurs only if the mass of the star allows the fusion. Smaller the mass, more the core has to be contracted to produce the required heat for next burning process to start. Further, the carbon then starts fusing into Neon to sustain against the force of gravity. The fusion reaction stops if there exists not enough pressure to support the gravitational force or the fusion reaction is not energetically favorable [Piz].

In case of a white dwarf (where the there exist a collection of atomic nuclei in a sea of electrons, kept apart by electron degeneracy pressure), the pressure-less and hence another fusion reaction is not possible. Whereas, if the mass of the star is more than $8M_0$, the fusion to further elements is energetically unfavorable after Iron (Fe^{56}) (being at the top of

the binding energy curve). In response, the core collapses, and there is a release of enormous amounts of gravitational energy with outer layer exploding outwards. Such process is termed as a type II supernovae explosion. Most of the stars with masses higher than $10M_0$ will result in a black hole. Only some with just enough mass to win the Pauli exclusion principle of electrons and sustained by the exclusion principle of neutrons will form Neutron Stars.

The crucial role in this explosion process is played by neutrinos which are trapped temporarily inside the star. They typically have a cross-section of $10^{40}cm^2$ and a mean free path of 10 cm (comparably less than the proto-neutron star radius of about 20km) [LP04]. Expanding remnant releases the kinetic energy of the order of 10^{51} erg. Finally, neutrinos and anti-neutrinos of all flavors are emitted in nearly equal proportions and carry a significant amount of energy outwards. Once the density in the core of the progenitor reaches around n_0, the collapse halts and a shock wave is produced at the outer edge. The shock wave loses its energy to the neutrinos and the nuclear dissociation of the material along the way. This loss in energy makes its path to be around 100 to 200km. Further, the pressure losses by the emission of neutrinos make the proto-neutron star to shrink faster.

Initially, due to the emission of neutrinos, the electron and proton combine and the matter inside becomes more neutron-rich. This process increases the temperature at the core. After 10 to 20 seconds, the steady emission of neutrinos starts to decrease the temperature at the inner core, and the star is able to cool. Now, the final core of matter produced after the proto-neutron star has cooled enough is called a stable neutron star.

1.2 First Observations and Properties

In 1934, the first proposal of the existence of neutron stars was made by Walter Baade and Fritz Zwicky. First proposed in order to explain the origin of supernovae. Jocelyn Bell first detected the highly magnetized, rapidly spinning neutron stars in the form of radio pulses which are known as radio pulsars. After its first observation, a total of about 2000 neutron stars in the Milky Way and the Magellanic Clouds have been observed, the majority of which have been detected as radio pulsars.

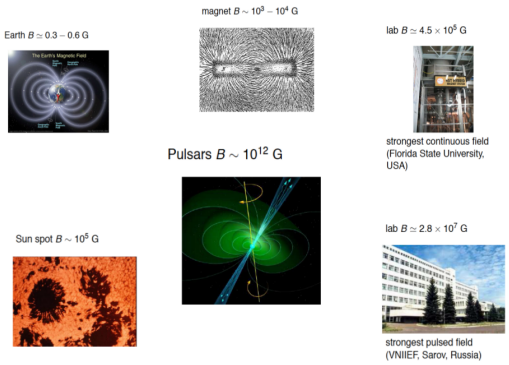

Figure 1.2: Lecture slides, The Equation of State for Neutron Stars by Laura Tolos

A typical neutron star has a mass of about $1.5M_0$ and a range of mass varying from $1-2M_0$. The most massive neutron star observed till date is the pulsar J0348+0432 with mass 2.01 $+/-$ $0.04M_0$ [ea13]. The central baryonic densities inside can vary from $5 - 10n_0$ where $n_0 \sim 0.16fm^{-3}$ is the saturation density of the nucleus. For comparison of the mass densities, one can estimate that the mass density of the whole universe is about 10^{-30} gcm^{-3} and the mass density of the earth is about 5.5 gcm^{-3}, whereas it is 5 to 10 times $3 * 10^{14}$ gcm^{-3} for a typical neutron star. The radius of neutron stars can range from 10 km to 15 km, and the typical radii are around 12 km. [LP15]

The neutron stars are observed as pulsars which are highly magnetized, rotating neutron stars. These pulsars emit a focused electromagnetic radiation in the form of jets through their magnetic axis. The misalignment between the magnetic axis and the spin axis leads to a 'lighthouse effect,' and hence pulses are observed from earth. The time period of pulses coming from the pulsars can vary from 10^{-3}s to 10s. These pulses are assigned as one of the most accurate clocks till date. The magnetic fields can vary from 10^8 G to 10^{16}G. For a comparison of the magnetic fields, see fig. 1.2.

Also, the temperature inside a newly formed neutron star is from around 10^{11} k to 10^{12} k. After the steady neutrino emission, the temperature comes down to nearly 10^6 Kelvin. Next chapter gives a detailed analysis of the states of matter present inside the structure of a neutron star at varying densities.

1.3 States of matter

In a neutron star, the state or the properties of matter in its ground state changes significantly with increasing density. The mass density from surface to core can vary from 10 gcm^{-3} to 10^{14} gcm^{-3}.

According to the cold catalyzed matter hypothesis, the matter inside a non-accreting neutron star is assumed to be in complete thermodynamic equilibrium with respect to all interactions at zero temperature. Hence, the matter is in its lowest possible energy state which is ground state configuration. At very low densities, the atmosphere of a neutron star is composed of atoms. The pressure at this stage is zero. This region continues for few ten's of cms inside the surface and the densities reach up to $10^4 gcm^{-3}$.

At $\rho \sim 10^4$ gcm^{-3}, Fe^{56} nuclei are arranged in the form of a lattice. The configuration for minimizing the Coulomb interaction energy is attained by a BCC lattice. This region accounts for the beginning of the outer crust of the neutron star. Further going inside, the densities increases due to the increase in gravitational pressure. For densities above $\rho \sim 10^4$ gcm^{-3}, the atoms become completely ionized, and the electrons become free. This is due to the beta decay reaction which occurs as an effect of increasing density, $n + p \rightarrow e^- + \overline{\nu_e}$. With the further increase in densities, the Fermi energy of electrons increases and the electrons become fully relativistic. The energy of the reaction can be depicted as : $m_n c^2 > m_e c^2 + m_p c^2 + E_e^F$.

At densities of about 10^7 gcm^{-3}, the electronic Fermi energy increases enough and it becomes energetically unfavourable for the beta decay reaction to occur due to a large sea of degenerate relativistic electrons ($m_n c^2 < m_e c^2 + m_p c^2 + E_e^F$). At this stage the protons and electrons began combining to form neutrons in an inverse beta decay reaction: $p + e^- \rightarrow n + \nu_e$. For $E_e^F \geq 1MeV$, the iron nuclei is not the most stable nuclei, and more neutron-rich nuclei begin to form. This process is termed as "neutronization." The sequence of neutron-rich nuclei which are formed in this process are Ni^{62},Ni^{64}, Se^{84}, Ge^{82}, Zn^{30}, Ge^{82}, Ni^{78}, Fe^{76}, Mo^{124}, Zr^{122}, Sr^{120}, Kr^{118}. These nuclei cannot be formed inside the laboratories on earth and are only found in neutron stars.

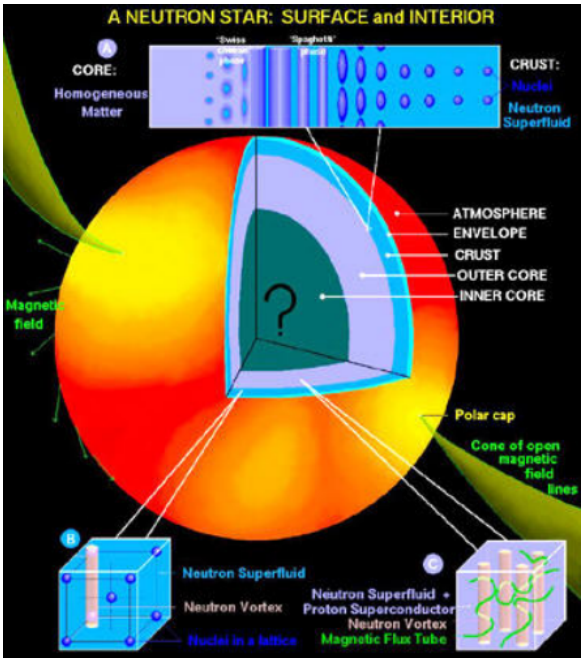

Figure 1.3: Internal Structure of a neutron star

At densities above $4.3 * 10^{11} gcm^{-3}$, the neutrons inside the nuclei increase so much that it is energetically more favorable for them to drip out of the nuclei. With further increase in mass density, the continuum neutron states begin to be populated and form a low-density sea of neutrons. This marks for the inner core of the outer crust of the neutron star structure. With increasing densities, the Fermi energy of neutrons begins to increase. All the states mentioned above account for the outer crust of the neutron star which ranges up to about 0.3 km inside from surface.

For densities between "neutron drip" and $2 * 10^{14} gcm^{-3}$, the matter consists of neutron-rich nuclei in a lattice and in addition, a gas of free neutrons as well as electrons penetrating the lattice. With higher densities, the nuclei and sea of neutrons, electrons, and protons began to take various structural forms due to the Colombic repulsion. These different structures of the form of rods and plates are known as "nuclear pasta"[DGRW83]. Starting with "meat-balls" which are 3-D structures of nuclei in a low-density sea of neutrons then a "spaghetti" phase with 2-D cylindrical nuclei in which thousands of nuclei are immersed in the liquid (or sea of free neutrons). Next phase is the "lasagna" phase, in which 1-D nuclei are left in the form of voids and sheets of nuclear matter is present. This is followed by "zitti" phase with 2-D structures cylindrical voids, then "swiss cheese" with 3-D voids and finally

a “sauce” with uniform nuclear matter and no nuclei are formed. This inner crust proceeds up to 0.6 km inside.

For densities of about $3 * 10^{14} gcm^{-3}$, the outer core begins to form which mainly consist of the uniform soup of sub-particles. The density in-homogeneity begins to smooth out and then disappears discontinuously in a first-order phase transition. A homogeneous liquid composed of neutrons, protons, electrons, muons, and possibly exotic matter, in - equilibrium, extends from the crust-core transition to the center of the star. For densities from $\rho_0/2$ to $2\rho_0$, the neutrons are able to form a ${}^3P_2$ superfluid. Migdal (1955) applied BCS theory to atomic nuclei to explain this superfluidity. Ginzburg and Kirzhnits (1964) then estimated the superfluidity gap produced by the singlet-state pairing of neutrons at the densities $\rho = 10^{13}$ to $10^{15} gcm^3$ and obtained gap, Δ of around 5 to 20 MeV. This superfluid consists of cooper pairs formed by neutrons due to the long-range attractive nuclear force; it is similar to the cooper pairs formed by electrons in a superconductor. The singlet-state neutron-neutron interaction becomes repulsive at supranuclear densities, and hence the interaction disappears at the core. Instead, low density of protons leads to the singlet-state proton-proton interaction which becomes attractive and can lead to proton pairing. Further, there is also a possibility of neutron pairing in the core due to the attractive part of the triplet-state neutron-neutron interaction.

In addition to exotic phases which can possibly appear at high densities, the matter may also be non-homogeneous in the core, e.g., a possible transition to a mixed phase involving hadrons and quarks can be achieved [NYT14]. For massive neutron stars with central mass density varying from 2 to 10 times ρ_0, a pure quark matter state can be achieved.

Chapter 2

Constraints

The macroscopic properties such as Mass and Radius of a neutron star can give significant insight on the states of matter present inside the crust and core of neutron star. By constraining the mass and radii values of a neutron star and determining the maximum mass of it, one can easily constrain the equation of state of the matter (see chapter 5). These constraints can come from various observables coming from the neutron star observations as well from widely known theoretical models.

2.1 Observational Constraints

The observations from Neutron star and their properties can be undertaken using several methods and techniques. The emission of photons from neutron stars results in the release of thermal energy. Considering them to be black body emitters, only measurements of fluxes, distances and temperatures can yield their radii. Some of these constraints are:
→ **pulsar timing:** to accurately measure the neutron star masses in compact binaries
→ **surface photon luminosity:** gives information about radius and thermal evolution
→ **X-ray bursts and superbursts:** give information about mass, radius and internal temperatures
→ **Supernova neutrinos:** tells us about the dense core
→ **Giant flare Quasi-Periodic Oscillations (QPO's):** tells us about the crust thickness and radius
→ **Gravity waves:** information on masses, mass-radius relation and details of the inspiraling orbit

2.2 Theoretical Constraints

There can be strong constraints on the mass and radius relations due to several well-established theories such as GR and thermodynamic relations.

2.2.1 General Relativistic Constraint

Neutron stars are such compact objects that general relativity (GR) is essential in determining their structure. But, they are not so dense that they form a black hole. This is due to the Pauli exclusion principle of fermions. Hence, the Fermi energy of neutrons prevents neutron stars to collapse into a singularity and form black holes. This argument can be used in a simple form, where one can set the limit that if the light does not escape from an object, it has to be a neutron star. In other words, if the potential energy of a compact object is less than the kinetic energy of a particle traveling with the speed of light, then it has to be a neutron star and not black hole. Consider the kinetic energy of a particle with mass, m moving with the speed of light, c as :

$$K = \frac{1}{2}mc^2 \tag{2.1}$$

Also, the potential energy of the compact object with mass, M, and radius, R can be written as:

$$U = \frac{GMm}{R} \tag{2.2}$$

Considering the limit to a neutron star as $k > U$, we can write:

$$\frac{1}{2}mc^2 = \frac{GMm}{R} \tag{2.3}$$

Therefore, we can easily have the constraint on the radius as:

$$R > 2\frac{GM}{c^2} \tag{2.4}$$

2.2.2 Uniform density star

The constraints due to hydrostatic equilibrium depend only on the relativistic pressure equations. Such constraint coming from the stability of matter demands that the rate of change

of pressure should always increase with mass density, i.e., $\frac{dP}{d\rho} > 0$ for all stars. This constraint applies to all kinds of star irrespective of the equation of state. But, an analytical solution of a uniform energy density star yields the exact same relation for the radius and hence has been discussed here. Neutron stars near their maximum mass do have a uniform density if not constant and do have incompressibility involved at high masses. So, even though the idealization seems hypothetical, it can have certain realistic factors involved in it [Gle97].

Considering a constant density, ϵ_0 throughout the star, the mass profile can be written as:

$$M(r) = \frac{4\pi}{3}\epsilon_0 r^3 \tag{2.5}$$

One integrates the equation of Hydrostatic equilibrium as given by relativistic theory and considers a constant density throughout to obtain:

$$\frac{p(r) + \epsilon_0}{3p(r) + \epsilon_0} = \sqrt{\frac{1 - \frac{2M}{R}}{1 + \frac{2Mr^2}{R^3}}} \tag{2.6}$$

Here, a boundary condition $p(R) = 0$ has been taken into account. Now, solving equation (3.6), one obtains:

$$\frac{2M}{R} = 1 - (\frac{p_c + \epsilon_0}{3p_c + \epsilon_0})^2 \tag{2.7}$$

Now, the larger the radius of a uniform density star, the more massive it is, and the higher the central pressure must be to support this mass. To constraint that the central pressure should not be high enough so that the maximum mass limit is maintained, the constraint can be put on eq. 2.7. Hence, taking a limit of large central pressure one have that get the required constraint as:

$$\frac{R}{M} > \frac{9}{4} \tag{2.8}$$

2.2.3 Causality Constraint

For an equation of state ($p(\rho)$) to be considered physically reasonable, the adiabatic speed of sound should not exceed the speed light i.e. $\frac{dP}{d\rho} < 1$ (considering c=1).
Considering the matter to be such that $p < \epsilon$, the limit on $\frac{2M}{R}$ becomes:

$$\frac{2M}{R} < \frac{3}{4} \tag{2.9}$$

Since the energy density of baryonic matter at low pressure is dominated by the rest mass of the baryons, any realistic equation of state must be in the domain $p < \epsilon$ at low pressure. For the matter to be ultrabaric, i.e., $p > \epsilon$, the causality constraint has to be broken. This limit is more specific to a uniform energy density star and not independently on the structural equations. However, it lies very close to a limit of 0.78 obtained by Bondi [HB64] under the reasonable assumptions concerning the equation of state.

Chapter 3

Structural Equations

This chapter briefly discusses the classical and relativistic theories required to derive the structural equations of a neutron star.

3.1 Newtonian Theory

According to classical theory, a star is thermodynamically stable or in equilibrium only if the gravitational attraction and the repulsion due to the energy generated inside it are balanced.

The gravitational force on a small mass element, dm (see 3.1) at a radius, r due to the object of mass m(r) can be written as:

$$dF = -\frac{G \cdot dm \cdot m(r)}{r^2} \tag{3.1}$$

where G is the gravitational constant with value $6.67408 \times 10^{-11} m^3 kg^{-1} s^{-2}$. Considering a mass density-dependent only on the radius of the compact object, we can write the differential mass as $dm = \rho(r) 4\pi r^2 dr$. The differential value of pressure on the mass element is described as $dp = \frac{dF}{4\pi r^2}$

Hence, substituting the values of force and mass, we get the differential equation for pressure:

$$\frac{dp}{dr} = -\frac{G \cdot \epsilon(r) \cdot m(r)}{c^2 r^2} \tag{3.2}$$

where $\epsilon(r)$ is the energy density defined as $\epsilon(r) = \rho(r) \cdot c^2$. Negative sign in this equation describes that the pressure values decrease with the increase in the radius from the center and becomes zero at the surface where $r = R$. Also, the mass variation in terms of energy

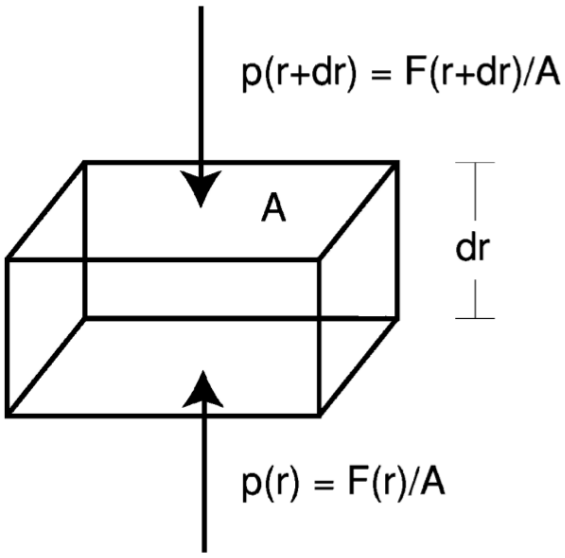

Figure 3.1: Neutron stars for undergraduates by Richard R. Silbar and Sanjay Reddy (2004)

density can be obtained from the given equation:

$$\frac{dm}{dr} = \frac{\epsilon(r) \cdot 4\pi r^2}{c^2} \tag{3.3}$$

By integrating the above equation, one can obtain the relation:

$$M(r) = 4\pi \int_0^r r^{'2} dr \rho(r^{'}) \tag{3.4}$$

In order to solve the equations (4.2), (4.3) and (4.4), we need to integrate from r=0 to r=R where R is the total radius of the star. The initial conditions required are $p(r = 0) = p_c$, R and M(R). To uniquely solve the equations an important requirement is the energy density profile, i.e., $\epsilon(r)$ in terms of the pressure profile, i.e., $p(r)$. This relation is known as the equation of state of the matter inside the star. A detailed description of the equation of states present in the neutron star is discussed in chapter 4.

This classical formulation works well only when the mass of a star is small and does not significantly "warp" the space-time which is the case for white dwarfs. But, the matter inside a neutron star is extremely dense and compact ($\frac{GM^2}{\frac{R}{Mc^2}} \sim 1$). Hence the structural equations required to develop the mass and pressure profiles inside a neutron star should depend on the curvature of space-time around it. The most widely used theory explaining the curvature of space-time is the theory of general relativity.

3.2 Relativistic Structural Equations

This section discusses, in brief, the basics of the general theory of relativity required to derive the structural equations of a neutron star.

3.2.1 Geometry of space-time

In Einstein's special and general theory of relativity, time is considered as a 4th dimension just like spatial ones. Therefore, for every point in space-time (called event) require four coordinates to be defined completely. The quantity which remains invariant to the choice of reference frame is useful in determining the physics. One such invariant quantity is the length of the four-dimensional vector between two events in space-time.
For a flat spacetime, the infinitesimal line element, ds is defined as:

$$ds^2 = (cdt)^2 - dx^2 - dy^2 - dz^2 \tag{3.5}$$

The flat space time metric, $\eta_{\mu\nu}$ describing the coefficients of the invariant, ds^2 as:

$$\eta^{\mu\nu} = \eta_{\mu\nu} = \begin{bmatrix} 1 & 0 & 0 & 0 \\ 0 & -1 & 0 & 0 \\ 0 & 0 & -1 & 0 \\ 0 & 0 & 0 & -1 \end{bmatrix} \tag{3.6}$$

Similarly, for a curved space-time with metric, $g_{\mu\nu}$ one can write the line element using the Einstein's summation convention as:

$$d\tau^2 \equiv ds^2 = g_{\mu\nu} dx^\mu dx^\nu \tag{3.7}$$

Where τ is the proper time measured in the frame of reference of a system. Now, the paths followed by freely moving particles is called a geodesic which is described by the geodesic equation as:

$$\frac{d^2x^\alpha}{d\tau^2} = -\Gamma^\alpha_{\beta\gamma} \frac{dx^\beta}{d\tau} \frac{dx^\alpha}{d\tau} \tag{3.8}$$

where $\Gamma^\alpha_{\beta\gamma}$ is called the Christoffel symbol, defined as:

$$g_{\alpha\delta}\Gamma^\delta_{\beta\gamma} = (\frac{\partial g_{\alpha\beta}}{\partial x^\gamma} + \frac{\partial g_{\alpha\gamma}}{\partial x^\beta} - \frac{\partial g_{\beta\gamma}}{\partial x^\alpha}) \tag{3.9}$$

Considering the addition of a new time dimension, the commonly used derivative is changed to *covariant derivative* defined as:

$$\Delta_\alpha \nu^\beta = \frac{\partial \nu^\beta}{\partial x^\alpha} + \Gamma^\beta_{\alpha\gamma} \nu^\gamma \tag{3.10}$$

The geodesic equation now can be written as: $\Delta_\alpha u^\alpha = 0$ where $u^\alpha = \frac{dx^\alpha}{d\tau}$. Now, the curvature in the fabric of space-time can be defined using a fourth rank tensor called *Riemann Curvature Tensor* defined as:

$$R^\alpha_{\beta\gamma\delta} = \frac{\partial\Gamma^\alpha_{\beta\delta}}{\partial x^\gamma} - \frac{\partial\Gamma^\alpha_{\beta\gamma}}{\partial x^\delta} + \Gamma^\alpha_{\gamma\epsilon}\Gamma^\epsilon_{\beta\delta} - \Gamma^\alpha_{\delta\epsilon}\Gamma^\epsilon_{\beta\gamma} \tag{3.11}$$

Another important second rank tensor called *Ricci curvature* is defined as:

$$R_{\alpha\beta} = R^\gamma_{\alpha\gamma\beta} \tag{3.12}$$

Ricci Scalor is then defined as:

$$R = g_{\alpha\beta}R^{\alpha\beta} \tag{3.13}$$

The distribution of energy and momentum in the space-time coordinates is given by the 4×4 second rank tensor called *stress-energy tensor*:

$$T_{\alpha\beta} = \begin{bmatrix} energy & density & energy & flux \\ momentum & density & momentum & flux \end{bmatrix} \tag{3.14}$$

After this background, the next section discusses the derivation of the structural equations which should be used for a neutron star.

3.3 Derivation

Considering only spherically symmetric systems, the metric can be written in terms of spherical coordinates. The generic form of metric can be written as:

$$g_{\mu\nu} = diag(e^{\nu(r)}, -e^{\lambda(r)}, -r^2, -r^2 sin^2\theta) \tag{3.15}$$

Here, g_{22} and g_{33} are the same as in a flat metric due to spherical symmetry. $\nu(r)$ and $\lambda(r)$ are the unknown functions which can be found from the constraints of isotropy in the stress-energy tensor. The Einstein's field equation with a cosmological constant, λ is given as:

$$G_{\alpha\beta} + \Lambda g_{\alpha\beta} = \frac{8\pi G}{c^4}T_{\alpha\beta} \tag{3.16}$$

where $G_{\alpha\beta} = R_{\alpha\beta} - \frac{1}{2}Rg_{\alpha\beta}$ in terms of Ricci curvature and Ricci scalar. Now, with the metric in equation 3.15, we can calculate the Einstein field tensor, $G_{\mu\nu}$. The stress-energy

tensor on the right-hand side of the equation must follow the conditions of isotropy, time-independence and spherical symmetry, giving it a form:

$$T^{\mu}_{\nu} = diag\big(\epsilon(r), -P(r), -P(r), -P(r)\big) \tag{3.17}$$

Now, to begin solving the Einstein's equations one require each component of the field tensor. Solving for G_{00}:

$$G_{00} = \frac{1}{r^2}[1 - \frac{d}{dr}\big(re^{-\lambda(r)}\big)]e^{\nu(r)} \tag{3.18}$$

Therefore, the first equation will be:

$$\frac{1}{r^2}[1 - \frac{d}{dr}\big(re^{-\lambda(r)}\big)]e^{\nu}(r) = ke^{\nu(r)}\epsilon(r) \tag{3.19}$$

Also, a shell with differential thickness, dr at a distance r from center will have mass as: $dM(r) = 4\pi\epsilon(r)r^2dr$ Substituting the value of $\epsilon(r)$ and integrating the equation 3.19 we get solution for g_{00}:

$$e^{-\lambda(r)} = 1 - \frac{k}{4\pi r}M(r) \tag{3.20}$$

Similarly, for G_{11} and T_{11}, the equation will be:

$$\frac{1}{r^2}\left(r\frac{d}{dr}\nu(r) - e^{\lambda(r)} + 1\right) = kP(r)e^{\lambda(r)} \tag{3.21}$$

Now, by substituting eq. (4.19) in eq. (4.20) one can solve for $\nu^{'}(r)$ as:

$$\nu^{`}(r) = \left(krP(r) + \frac{k}{4\pi r^2}M(r)\right)\left(1 - \frac{k}{4\pi r}M(r)\right)^{-1} \tag{3.22}$$

Another relation for $\nu^{`}(r)$ can be obtained from the conservation of energy-momentum tensor ($\Delta_{\mu}T^{\mu}_{1} = 0$):

$$\nu^{`}(r) = -2\frac{dP(r)}{dr}\frac{1}{P(r) + \epsilon(r)} \tag{3.23}$$

Now, comparing equations 3.22 and 3.23 along with the unit of c and G, we obtain:

$$\frac{dP(r)}{dr} = -\frac{G\epsilon(r)M(r)}{r^2c^2}\left(\frac{P(r)}{\epsilon(r)} + 1\right)\left(\frac{4\pi r^3P(r)}{c^2M(r)} + 1\right)\left(1 - \frac{2GM(r)}{c^2r}\right)^{-1} \tag{3.24}$$

Another relation with mass variation is given as:

$$\frac{dM(r)}{dr} = 4\pi\frac{\epsilon(r)}{c^2}r^2 \tag{3.25}$$

Both, equations 3.24 and 3.25 combined are known as **Tolmann-Oppenheimer-Volkoff equation** (TOV equation). One can see dimensionally that in equation (4.24), the correction due to the special theory of relativity is in the first 2nd and 3rd terms. Pressure varies

as $k_F^2/2m = mv^2/2$ and energy density varies as mc^2. This effectively makes the ratio of pressure and energy density ($\sim \frac{v^2}{c^2}$) vanish as one goes to the classical regime. The last term gives the correction from general relativity as it takes into account the compactness of the object, i.e., $\frac{GM}{Rc^2}$.

To solve these TOV equations and find the mass and pressure profile of the complete neutron star structure, it is required that we know the relation of pressure with energy density. This relation of $P(\rho)$ is called the equation of state of the matter and is characteristic of the type of matter present inside a neutron star.

Since, in a neutron star, there exist different types of matter as one goes to higher and higher densities in its internal structure; hence a single equation of state cannot be used to solve the TOV equations (refer to chapter 4).

3.4 Dimensionless equation

This section discusses the process of making the TOV equations dimensionless, which makes it easier to use in numerical codes. To write the TOV equations in a form which can be read in physically acceptable units, one can first make the mass in terms of the units of solar masses (M_0). Therefore, we can transform the relations as:

$$\overline{M} = \frac{M(r)}{M_0} \tag{3.26}$$

Using this relation, mass differential equation becomes:

$$\frac{d\overline{M}(r)}{dr} = \frac{4\pi\epsilon_0}{M_0 c^2}\frac{\epsilon(r)}{\epsilon_0}r^2 \tag{3.27}$$

where ϵ_0 is introduced to make the energy density dimensionless such that:

$$\overline{\epsilon} = \frac{\epsilon(r)}{\epsilon_0} \tag{3.28}$$

The dimension of ϵ_0 is that of energy density given as $\frac{m^4c^5}{\pi^2\overline{h}^3}$. Another dimensionless quantity can be introduced as:

$$\beta = \frac{4\pi\epsilon_0}{M_0 c^2} \tag{3.29}$$

The first TOV equation becomes:

$$\frac{d\overline{M}(r)}{dr} = \beta r^2 \overline{\epsilon} \tag{3.30}$$

Similarly, we can make pressure dimensionless by introducing the relation:

$$\overline{P} = \frac{P(r)}{\epsilon_0} \tag{3.31}$$

Using relations 3.26, 3.28 and 3.31 in the TOV equation 3.24, one obtain the dimensionless form as:

$$\frac{dP(r)}{dr} = -\frac{\overline{\epsilon}(r)\overline{M}(r)R_0}{r^2}\left(\frac{\overline{P}(r)}{\overline{\epsilon}(r)} + 1\right)\left(\frac{\beta r^3 \overline{P}(r)}{\overline{M}(r)} + 1\right)\left(1 - \frac{2R_0\overline{M}(r)}{r}\right)^{-1} \tag{3.32}$$

where R_0 is half the Schwarzschild radius of the sun, i.e., $\frac{GM_0}{c^2}$
The equations 3.30 and 3.32 along with the relation of pressure with energy density called 'equation of state' of the matter, can be used in numerical codes to obtain the mass and pressure profiles in physically acceptable units. This system of three equations can be solved analytically for some simple cases and numerically otherwise.

In the next chapter, various equations of states and their implications on the macroscopic properties such as mass and radius are discussed. The basic cases of constant density, non-relativistic and ultra-relativistic Fermi gas and further various other widely used EOS's are considered analytically (if possible) as well as numerically.

Chapter 4

Equation of States

The relation of pressure at any stage in a system with the energy or mass density of the system is called the **'Equation of State'** of the system. This relation is characteristic of the type of matter present in its ground state and hence depicts the properties of such matter.

The TOV equations require the equation of state to solve the structure of neutron star uniquely, hence it is important to predict what kind of matter can be present. Further sections discuss several equations of state models which are used to evolve the structure.

4.1 Constant density model

One simple model which can be used to solve the equation is that of the constant density model. In this type of star, the energy density all throughout the star is assumed to be constant. Such a star is in-compressible in structure and hence closer to realistic EOS.

Now, when the energy density is constant (say ϵ_0) one can write the equation 3.25 as $\frac{dM}{dr} = \frac{4\pi\epsilon_0 r^2}{c^2}$ One can hence find the value of mass as a function of radius by integrating the equation from r'=0 to r'=r:

$$M(r) = \frac{4\pi r^3}{3}\frac{\epsilon_0}{c^2} \tag{4.1}$$

The profile of mass is obtained using python for constant mass density ($\rho = 3\times10^{17} kgm^{-3}$), see figure 4.1. Further, substituting this equation in 3.24, we get:

$$\frac{dp}{dr} = -\frac{G\epsilon_0(\frac{4\pi r^3}{3}\frac{\epsilon_0}{c^2})}{r^2c^2}\left(\frac{P(r)}{\epsilon_0}+1\right)\left(\frac{4\pi r^3 P(r)}{c^2(\frac{4\pi r^3}{3}\frac{\epsilon_0}{c^2})}+1\right)\left(1-\frac{2G(\frac{4\pi r^3}{3}\frac{\epsilon_0}{c^2})}{c^2 r}\right)^{-1} \tag{4.2}$$

After solving the equation one gets:

$$\frac{dP(r)}{dr} = -\frac{4\pi rG}{3c^4}\frac{(p+\epsilon_0)(3p+\epsilon_0)}{1-(\frac{8\pi r^2\epsilon_0 G}{3c^4})} \tag{4.3}$$

Integrating the equation from r=0 to r=R, using boundary conditions as:

$$p(r=0) = p_c; p(r=R) = P \tag{4.4}$$

where p_c is the initial pressure at the centre of neutron star, one will get the relation of total radius as:

$$R^2 = \frac{3c^4}{8\pi\epsilon_0 G}\Big[1 - \Big(\frac{(3P+\epsilon_0)(p_c+\epsilon_0)}{(P+\epsilon_0)(3p_c+\epsilon_0)}\Big)^2\Big] \tag{4.5}$$

Now, assuming that the pressure at the surface is zero as the approximation is useful compared to the pressures at the core ($\sim 10^{35}$ Pa), we get:

$$R^2 = \frac{3c^4}{8\pi\epsilon_0 G}\Big[1 - \Big(\frac{(p_c+\epsilon_0)}{(3p_c+\epsilon_0)}\Big)^2\Big] \tag{4.6}$$

Now, by solving the derivative of the R^2 with respect to p_c, we can obtain the maximum radius for a given central pressure:

$$\frac{dR^2}{dp_c} = \frac{12c^4}{8\pi\epsilon_0 G}\frac{(\epsilon_0+p_c)(\epsilon_0)}{(\epsilon_0+3p_c)^3} = 0; \tag{4.7}$$

This gives a limit of $p_c \to \infty$, for a maximum radius. Hence the value of maximum radius which depends only on the constant density throughout is given as:

$$R_{max} = \frac{c^4}{3\pi\epsilon_0 G} \tag{4.8}$$

Using the radius given in Eq. 4.6, one can easily solve for mass with equation 4.1. One can find the relationship of the radius with mass by substituting for mass in the equation above:

$$R = \frac{2GM}{c^2}\Big(1 - \frac{(p_c+\epsilon_0)^2}{(3p_c+\epsilon_0)^2}\Big) \tag{4.9}$$

Hence, the initial conditions of p_c and ϵ_0 give us the value of the total radius of the neutron star.

Similarly, the relation of pressure with radius can be obtained from the equations as:

$$P = \epsilon_0\left[\frac{\Big(1-\frac{8\pi r^2\epsilon_0 G}{3c^4}\Big)^{\frac{1}{2}}\Big(\frac{3p_c+\epsilon_0}{p_c+\epsilon_0}\Big) - 1}{3 - \Big(1-\frac{8\pi r^2\epsilon_0 G}{3c^4}\Big)^{\frac{1}{2}}\Big(\frac{3p_c+\epsilon_0}{p_c+\epsilon_0}\Big)}\right] \tag{4.10}$$

In order to solve the Tolman-Oppenheimer-Volkoff equations, a code is developed in C++

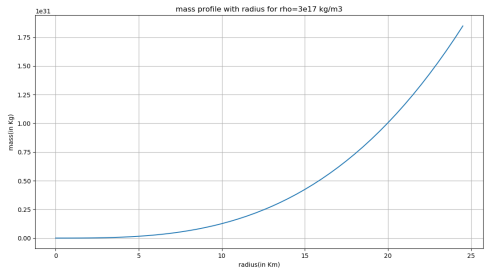

Figure 4.1: Plot of Mass profile with Radius using the analytical relation (see eq. 4.1) using Python

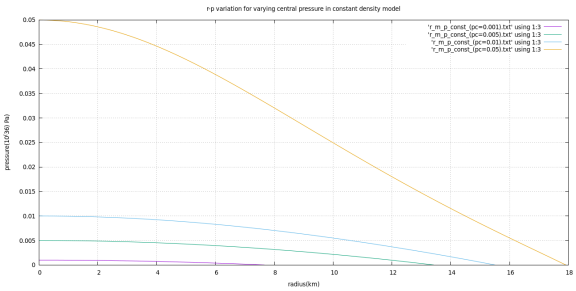

Figure 4.2: Plot of pressure profile with radius for different central pressures by solving TOV equations (4.1,4.2) in C++ code)

which takes the initial conditions for mass ($m = 0.0$) and pressure ($p = p_c$) at the center of neutron star. It then use Runge-Kutta-4th order method to solve the two differential equations. In the case of a constant density star, the energy density is taken to be constant and a plot of pressure profile with radius is made (see fig. 4.2). Also, the plot for total mass and radius of stable neutron stars can be seen in fig. 4.3. We can see that the total mass can go upto any value depending on the central pressure values and restricted by the maximum radius relation (eq. 4.8).

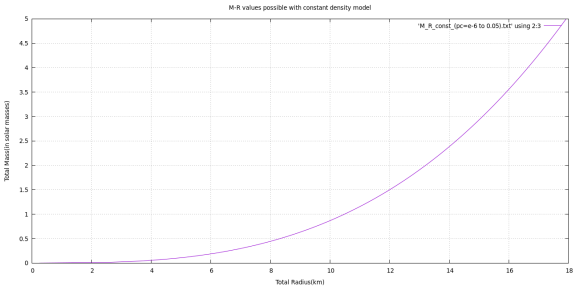

Figure 4.3: Plot of Total Mass with Total Radius of stable neutron stars, obtained by solving TOV eqs. (4.1,4.2)

4.2 Fermi-Gas Approximation

A better approximation would be to assume a neutron star to sustain on the degeneracy pressure of the neutrons which is due to the Pauli Exclusion Principle. Such case is possible only due to the fermionic nature of neutrons. Hence, the Fermi-gas approximation can be taken with the distribution given as:

$$n(\epsilon) = \frac{1}{e^{\frac{(E-\mu)}{k_B T}} + 1} \tag{4.11}$$

where E is the energy of particle, μ is the chemical potential and T is the temperature.

In the next subsection, relations of pressures, fermi-energies and internal energies have been derived for both non-relativistic and relativistic cases.

4.2.1 Degeneracy pressure for a non-relativistic and relativistic gas

Full degeneracy is the case when all the lowest energy quantum states are completely filled at low temperatures. Therefore, in full degeneracy, the Fermi/degeneracy pressure is non-zero even at absolute zero temperature, which should be the case for a neutron star. In such case, adding more particles to the system of decreasing the volume of the system results in the filling of higher energy states. This in effect, requires a compression force which is felt as resisting while adding particles. Such degeneracy pressure does not depend on the temperature of the system and only depends on the density of fermions. Therefore, dense stars remain in complete equilibrium independent of the thermal structure inside.

At absolute zero temperature, all the energy states of Fermi sphere are occupied. Hence we can write the total number of occupied cells as:

$$N = \frac{\frac{4\pi p_F^3}{3}}{\frac{h^3}{V}} \tag{4.12}$$

where p_F is the fermi pressure and V is the volume of elementary block in real space. Solving this equation we can get the fermi pressure in terms of number density (i.e. $\frac{N}{V}$):

$$p_F = \left(\frac{N}{V}\right)^{\frac{1}{3}} \left(\frac{3h^3}{8\pi}\right)^{\frac{1}{3}} \tag{4.13}$$

The above equation is valid for non-relativistic as well as relativistic cases as no mass term is involved.

Non-Relativistic Case The fermi energy can be obtained using the Newtonian relation, $E_F = \frac{p_F^2}{2m}$ and substituting p_F, we get:

$$E_F = \left(\frac{N}{V}\right)^{\frac{2}{3}} \left(\frac{3h^3}{8\pi}\right)^{\frac{2}{3}} \frac{1}{2m} \tag{4.14}$$

Now, the internal energy ($N \times E_F$) which is the total energy of the system can be written as:

$$E_{int} = \left(\frac{3h^3}{8\pi}\right)^{\frac{2}{3}} \frac{V}{2m} \left(\frac{N}{V}\right)^{\frac{5}{3}} \tag{4.15}$$

hence, the total pressure exerted by the particles in the system is $P = \frac{2E_{int}}{3V}$, by substituting we get,

$$P_{deg}^{non-rel} = \left(\frac{3h^3}{8\pi}\right)^{\frac{2}{3}} \frac{1}{3m} \left(\frac{N}{V}\right)^{\frac{5}{3}} \tag{4.16}$$

This relation of pressure with number density can be easily converted to the relation with mass density and the dependence remains same, i.e. $P \propto \rho^{\frac{5}{3}}$

This approximation is good only if the density of the system remains low. As the particles come closer and the system is more compressed, the particle's position uncertainties becomes less, and hence according to Heisenberg's uncertainty principle ($\Delta x \cdot \Delta p \geq \frac{h}{2\pi}$) the particle's momentum uncertainty becomes extremely high, resulting into large velocities. Therefore, even though the plasma is cold, the particles are moving extremely fast. Newtonian theory is not a good approximation to handle such large velocities and hence a relativistic model for the degenerate fermi-gas has to be used for neutron stars.

The TOV equations 3.24, 3.25 have been solved using the equation of state in eq. 4.16 and the profiles of mass and pressure with radius are obtained (see figs. 4.4,4.5). Further, the relation of total mass with radius for stable neutron star is obtained with varying central pressures (see fig. 4.6). The maximum mass is obtained to be $0.96M_0$, which is about one solar masses away from the currently observed value of about $2.01M_0$. Also, the mass variation with central pressures can be seen from fig. 4.7.

Relativistic Approximation The relation for fermi pressure as given in eq. 4.13 remains the same in relativistic approximation. The fermi energy can now be given by the Einsteins relation, $E_F^2 = m^2c^2 + p_F^2c^2$. Considering the ultra-relativistic case, we can remove the

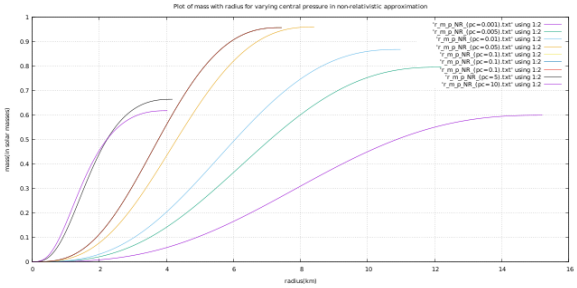

Figure 4.4: Plot of Mass with Radius of stable neutron stars for non-relativistic approximation of fermi-gas model, obtained by solving TOV eqs. (3.24,3.25)

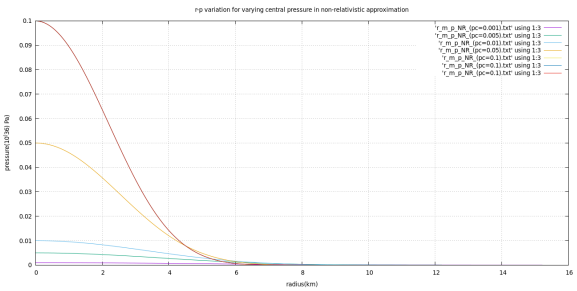

Figure 4.5: Plot of Pressure with Radius of stable neutron stars for non-relativistic approximation of fermi-gas model, obtained by solving TOV eqs. (3.24,3.25)

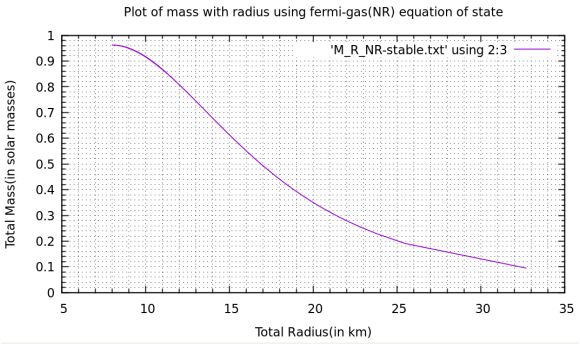

Figure 4.6: Plot of Total Mass with Total Radius of stable neutron stars for non-relativistic approximation of fermi-gas model, obtained by solving TOV eqs. (3.24,3.25)

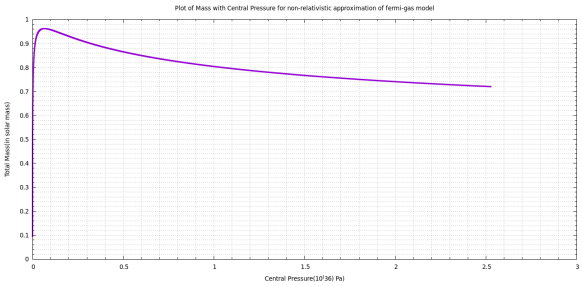

Figure 4.7: Plot of Total Mass with Central Pressures of stable neutron stars, obtained by solving TOV eqs. (3.24,3.25)

mass term and substitute for p_F to obtain,

$$E_F = \left(\frac{N}{V}\right)^{\frac{1}{3}} \left(\frac{3}{8\pi}\right)^{\frac{1}{3}} hc \tag{4.17}$$

Hence, the total energy of the system can be found by integrating the fermi sphere as:

$$E_{total} = \frac{2}{h^3} \int d^3r \int d^3p(pc) \tag{4.18}$$

Resulting into the expression:

$$E_{total} = \frac{3}{4}\left(\frac{3}{8\pi}\right)^{\frac{1}{3}} (Vhc)\left(\frac{N}{V}\right)^{\frac{4}{3}} \tag{4.19}$$

Also, the total pressure exerted by the particles on the system is obtained by the thermodynamic equation, $P = -(\frac{\partial E}{\partial V})_N$,

$$P_{deg}^{rel} = \left(\frac{3}{\pi}\right)^{\frac{1}{3}} \left(\frac{hc}{8}\right)\left(\frac{N}{V}\right)^{\frac{4}{3}} \tag{4.20}$$

Above equation reflects the dependence of density on the pressure of an ultra-relativistic degenerate fermi-gas. Comparing the proportionality on the mass as well as number density in the equations:

$$\begin{aligned} P_{deg}^{non-rel} &\propto \rho^{\frac{5}{3}}, \\ P_{deg}^{rel} &\propto \rho^{\frac{4}{3}} \end{aligned} \tag{4.21}$$

We can see that the exponent of the above equations should have different implications on the overall structure of the neutron star. Such various implications of the different equation of states can be used to categorize the equation of states into two different categories, soft and stiff. These categories are relative, and the equations can be labeled one or the other kind only when compared.

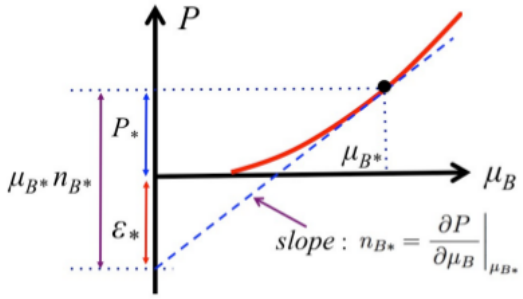

Figure 4.8: Graphical analysis of the equation of state, P (μ_B). The slope of the tangent line a given point (μ_B^*,P^*), is the baryon density, n_B^* , and its intercept on the P axis is the negative of the energy density ϵ^*[BHT18]

Soft and Stiff Equation Of States

A soft equation of state is the one in which for a given energy density, ϵ (or mass density, $\rho = \epsilon/c^2$), the pressure is less compared to the other. This can be interpreted as a lesser increase in the value of pressure for a given increase in the density. Such relation would imply high compressibility (i.e., easier to compress) of the matter and hence a lower neutron star mass when used in TOV equations.

Whereas, for a stiff equation of state, the pressure is strongly dependent on the change in the value of mass or energy density, implying lesser compressibility and hence a higher value of the total mass of neutron star. If $P \propto \rho^{\Gamma}$, the softness, and stiffness of the equation can be easily determined from the low (soft) and high (stiff) value of the exponent Γ.

Another interpretation of the same can be seen from the geometrical perspective (see fig. 4.8). Considering the thermodynamic relation (at zero temperature) of pressure with energy density,

$$P = \mu_B n_B - \epsilon \tag{4.22}$$

where μ_B is the baryonic chemical potential and n_B is the baryonic number density. The EOS here can be taken as a relation of P with μ_B and same implications can be extended as above. The slope of the graph will be $\frac{\partial P}{\partial \mu_B} = n_B$. The smaller the slope of P at given μ_B, the stiffer the equation of state. Similarly, the smaller is μ_B for a given P and slope, the stiffer is the equation of state, as shown in Fig.4.9

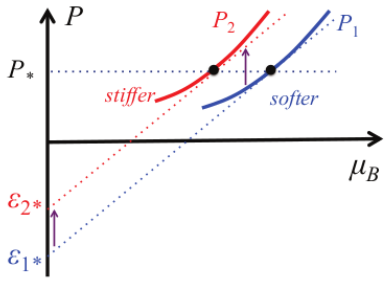

Figure 4.9: Comparing two EOS, pressure curves have same shape but P_2 is shifted towards lower chemical potential relative to P_1. P_2 is stiffer than P_1 because $\epsilon_1^* > \epsilon_2^*$

Hence, looking at equation 4.21, we can say that the ultra-relativistic approximation to the fermi gas model of neutrons is softer than the non-relativistic assumption of the equation of state.

4.3 Baym-Pethick-Sutherland Model

In this model, the equation of state for the matter in nuclear equilibrium at zero temperature is calculated for mass densities below $5 \times 10^{14} gcm^{-3}$. To determine the EOS for densities from 10^4 to $4.3 \times 10^{11} gcm^{-3}$ (neutron drip point), the effect of Coulomb lattice have been taken into account and the corresponding equilibrium nuclides are found using extrapolations from nuclear masses [Bay71a]. Further, from densities $4.3 \times 10^{11} gcm^{-3}$ to $5 \times 10^{14} gm^{-3}$, Baym, Bethe, Pethick (BBP) [BBP71] EOS has been used along with the EOS by Pandharipande [Pan71] (including the effect of hyperons) for higher densities.

The densities used to describe the state are found only in the outer crust of a neutron star. As mentioned in the introduction, for densities above $10^4 gcm^{-3}$, free neutrons begin to appear stabilizing against beta-decay, and the equilibrium nuclide is increasingly neutron-rich. Hence, the equation of state is found only after determining which nuclide is present at the respective densities.

The energy in such state mainly comprises three factors, nuclear energy, free electron energy and the lattice energy (negative). A competition between nuclear surface energy (favors nuclei with a higher number of nucleons, A) and Coulomb energy (favors small A

nuclei), decides the equilibrium nuclide. Coulomb energy includes a positive contribution from nuclear coulomb self-energy and a negative contribution from the lattice coulomb energy. At densities of about $2 \times 10^{11} gcm^{-3}$, the lattice contribution reduces about 15% of the net Coulomb energy. This significant effect is taken into account while calculating the nuclide and hence their equation of state.

For densities above $10^{11} gcm^{-3}$, the BBP model which describes the nuclei by a compressible liquid model is extended to include the lattice coulomb contributions as they become almost the same as the nuclear coulomb effects in such regimes.

The total energy of the system per unit volume before neutron drip,

$$E_{tot} = n_N(W_N + W_L) + E_e(n_e) \tag{4.23}$$

where $W_L(A, Z)$ is the lattice energy per nucleus (depending on mass and atomic number), W_N is the total energy of an isolated nucleus, E_e is the electronic energy per unit volume and n_N is the number of nuclei per unit volume. The lattice energy is minimized for a body-centered cubic (BCC) lattice and is given by the expression, $W_L = -1.819620 Z^2 e^2/a$ where $a = (2/n_N)^{1/3}$ is the lattice constant.

Above $10^4 gcm^{-3}$, the electrons can be considered free and the electronic energy density can be given as:

$$E_e = \int_0^{k_e} \frac{k^2 dk}{\pi^2} c(\hbar^2 k^2 + m_e^2 c^2)^{\frac{1}{2}} \tag{4.24}$$

Now, the equilibrium nucleus (or the equilibrium values of A and Z) can be found by minimizing the total energy density, E_{tot} at fixed baryon density, n_b.

But, this method of finding equilibrium nuclei involves density discontinuities every time a transition from one nucleus to other nucleus occurs. Hence, to avoid this discontinuity, one can take pressure as an independent variable instead of baryon density. Therefore, by minimizing the chemical potential at a fixed pressure, the equilibrium A and Z values can be obtained. The baryon chemical potential is given as:

$$\mu \approx \frac{E_{tot} + P}{n_b} \tag{4.25}$$

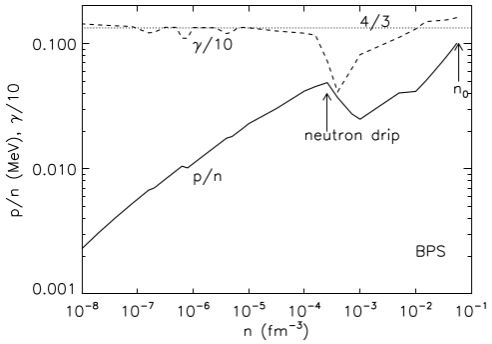

Figure 4.10: The BPS EOS is shown, the solid line is the pressure and the dashed line is the polytropic exponent. The value corresponding to $\gamma = 4/3$ (i.e. relativistic case) is shown as the dotted line. The neutron drip density and the core-crust transition density n_0 are shown.

Now, the pressure is given by thermodynamic relation, $\frac{\partial(E_{tot}/n_b)}{\partial n_b}\Big|_{Z,A}$ which on substituting E_{tot} from eq. 4.23 can be written as:

$$P = P_e + \frac{1}{3} W_L n_N \tag{4.26}$$

where $P_e = n_e \frac{\partial E_e}{\partial n_e} - E_e$ is the electron pressure and the second term can be taken as the negative pressure contribution due to lattice coulomb energy. Therefore, the chemical potential to minimize to find the equilibrium nuclei can be written as:

$$\mu = (W_N + \frac{4}{3} W_L + Z\mu_e)/A \tag{4.27}$$

Finally, the equation of state can be found in the following manner. At a particular value of pressure, one can find the electronic pressure contribution, P_e using Eq. 4.26. The measure of P_e can easily give the free electron momentum using the thermodynamic definition of P_e and hence the electronic energy can be found using the relation 4.24. Lastly, the electronic energy contribution can give the total energy density of the system using Eq. 4.23. Following this method for each of the nuclei available (A, Z values), we will get the entire equation of state for the crust region.

The equation of state in such model is shown in fig. 4.10 where a comparison can be seen with the relativistic approximation of Fermi-gas model.

This model has been taken to solve the TOV equations, and the mass and pressure profiles are found out. A plot of masses with varying central pressures if obtained (see fig. 4.12). Further, the stable values of Total Mass and Pressure for which the neutron star exists are

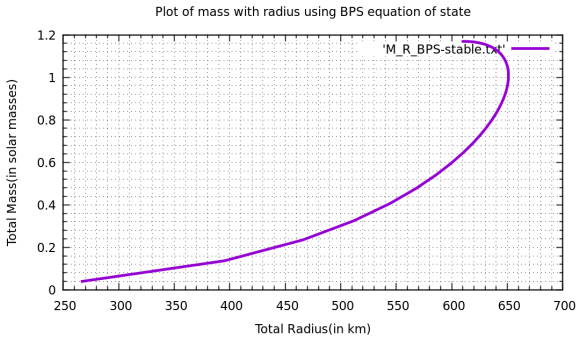

Figure 4.11: Plot of Mass with Radius for varying central pressures of stable neutron stars for BPS model, obtained by solving TOV eqs. (3.24,3.25)

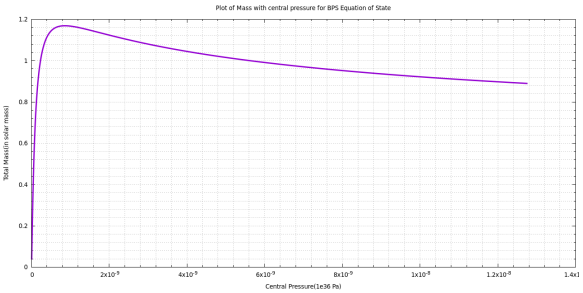

Figure 4.12: Plot of Mass with Central Pressure of stable neutron stars for BPS model, obtained by solving TOV eqs. (3.24,3.25)

estimated and developed in the plot (see fig. 4.11). The maximum mass is found to be about $1.16M_0$. This value is closer to the observed $2.01M_0$ limit of the neutron star as compared to the Fermi-gas model but still lacks the accuracy. Next section includes the symmetry energy contribution of the nucleons present at high densities.

4.4 Symmetry Energy Calculations

For densities above neutron drip (i.e from n_0 to $2n_s$), the matter is a structure-less fluid of nucleons. Due to charge fractions of proton and neutron present in such state, one can find the EOS by minimizing the total energy per baryon with respect to charge fraction, x($= n_p/n_n$) where n_p and n_n are the respective proton and neutron fraction. The energy with proton fraction, x can be estimated by relation:

$$E(n, x) \equiv E_{1/2}(n) + S(n)(1 - 2x)^2 \tag{4.28}$$

where $n = n_n + n_p$, S(n) is the nuclear symmetry energy defined as the difference in the energies of symmetric matter and pure neutron matter and $E_{1/2}(n)$ is the energy per

baryon of symmetric matter (defined as -16MeV by Lattimer'16 [LP16]). Another term for symmetry energy can be used if the quadratic approximation is applicable,

$$S_2(n) = (1/8)(\partial^2 E(n,x)/\partial x^2)_{x=1/2} \tag{4.29}$$

Near n_s, the symmetry energy can be written as $S(n) = S_\nu(n/n_s)^\gamma$, where $S_\nu = S_2(n_s)$ with value ranging from 26 to 34 MeV and γ between 0.3 to 0.7 according to recent calculations [LP16]. The pressure in terms of baryon number and proton fraction can be writen as

$$p(n,x) = n^2\frac{\partial E}{\partial n} \approx p_{1/2}(n) + S_\nu\gamma n_s(\frac{n}{n_s})^{\gamma+1}(1-2x)^2 \tag{4.30}$$

New calculations [GCR12] can be used to produce double power law of energy,

$$E(n,0) = a(n/n_s)^\alpha + b(n/n_s)^\beta \tag{4.31}$$

where a,b,α and β are estimated from quantum Monte Carlo neutron matter calculations [GCR12]. For densities above $2n_s$, the same methods cannot be extrapolated using TOV equations as the observed maximum masses are too low and do not comply with the observed neutron stars of masses about $2.01M_0$. Hence, the strong interaction between particle explained by field theory models is required to obtain accurate results.

The involvement of protons, electrons, and heavy leptons at high densities marks the importance of strong force with which they interact (note that Fermi-gas model does not take into account the interaction between neutrons) and these interactions must modify the equation of state of the system. The strong force can be easily described using the relativistic mean-field (RMF) models in which the exchange particles are massive spin zero and spin one mesons.

In σ-ω model by Chin and Walecka [CW74], neutrons and protons are treated as a single particle with each of them as a possible state, nucleon. The strong force in this model is mediated by two massive mesons, σ, and ω. Further, quantum chromodynamics (QCD) is the most acceptable theory which describes the strong force interactions. This thesis work mainly focuses on using the equation of states developed by such models and interpolating them with other lower density models (such as BPS, BBP, etc.) to finally develop a mass-radius relationship for neutron stars along with determining the maximum stable neutron

star mass.

The recent discovery of a massive binary pulsar (J0348+0432) with mass, $2.01+/-0.04M_0$ has put doubts on many hadronic theories. Such high mass requires stiff equation of state of the matter in a neutron star, and hence many theories such as the existence of hyperons (which soften the equation of state) in the core are ruled out. Such requirement of stiff EOS can impose strong constraints on the phases of QCD matter.

For massive neutron stars with densities above $2n_s$, the matter begins to melt, and the hadrons lose their identity into 'De-confined' quark matter. Such quark phase if present in a neutron star would have significant implications on the macroscopic properties such as mass and radius and could result in the correct predictions.

4.5 High density states and phase transitions

The different phases of matter present at extreme values of temperature and baryon densities are given by the fig. 4.13

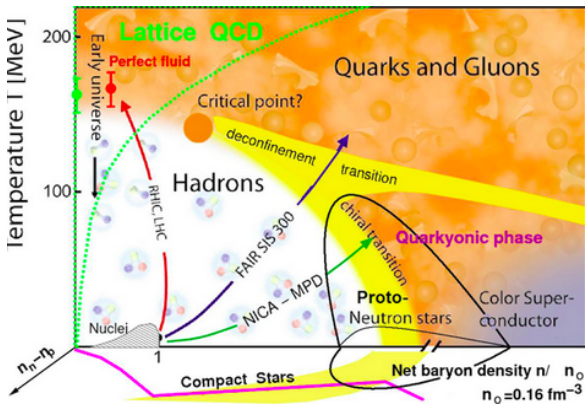

Figure 4.13: Plot of temperature with baryon densities

For low temperatures (below 150 MeV) and low chemical potential (or low densities), the hadronic degrees of freedom are present, and particles such as neutrons, protons, mesons in their confined structure are found in stable equilibrium. At extremely high temperatures or high chemical potential, hadrons start to become de-confined, i.e., hadrons lose their identity and form quark-gluon plasma with the fundamental degrees of freedom are quarks and gluons.

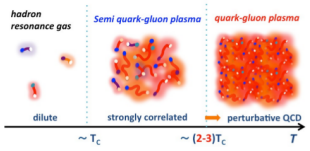

Phase transition at high temperatures [BHK+17]

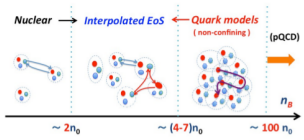

Phase transition at high baryon density (as occur in neutron stars) [BHK+17]

In neutron stars, the temperatures at the core are smaller than the ranges (10 to 200 MeV) present in the figure, whereas due to their extreme compactness and high densities, the chemical potentials go up to several times the saturation densities. We can see that neutron stars lie on the flat axis of baryon densities with nearly zero temperature (comparably). Hence, the phase transition from hadronic phase to the quark-gluon plasma can occur by two methods as shown in figure 4.5 and figure 4.5.

At low temperatures, dilute gas of hadrons is present, with the increase in temperature (as shown in fig 4.5) to around T_c, the hadrons start to melt, and the structure of matter present keeps on transforming to form a mixed phase. In this range from T_c to $2T_c$, the proper quasi-particle description of quarks and gluons is not applicable as even though the hadrons lose their structure, the strong correlations between quarks are present and hence the system is described as "semi-QGP." The transition process is very smooth and is described by lattice Monte Carlo calculations. Further for higher densities, the perturbative QCD calculations (which are mainly applicable beyond $(2-3)T_c$) can be extended in the crossover picture as many similar features are found in the transition phase.

Whereas, the quark matter can be composed at high baryon density and low temperatures (in neutron stars) as shown in fig. 4.6. In such case, for densities up to $2n_0$, the interactions occur through meson or quark exchanges and the RMF theory discussed above is valid. For densities $2n_0 < n_B < (4-7)n_0$, the quark exchanges increase gradually and are able to propagate throughout the system and hence the system changes from hadronic matter to quark matter (this is described by percolation theory). In this regime, an interpolated EOS can be used to match with low and high-density EOS's. For densities above $(4-7)n_B$, the quarks no longer belong to their specific baryons, and perturbative QCD model can be applied.

The presence of quarks and gluon degree of freedom in the intermediate densities ($(2-4)n_0$) require phenomenological modeling and a complete understanding of the quark matter present at much higher densities so that proper interpolations can be made.

4.5.1 Quark matter

Considering the degenerate Fermi sea of massless quarks at low temperatures, one can write the density of quarks as,

$$n_q = 2N_cN_f \int_0^{p_F} \frac{d^3p}{2\pi^3} = N_cN_f \frac{p_F^3}{3\pi^2} \tag{4.32}$$

where N_c and N_f is the number of quark colors (3) and flavors and p_F is the quark fermi momentum. The quark kinetic energy density can be written as:

$$\epsilon_k = 2N_cN_f \int_0^{p_F} \frac{d^3p}{2\pi^3}|p| = N_cN_f \frac{p_F^4}{4\pi^2} \tag{4.33}$$

Now, the total energy density, ϵ $(= \epsilon_k + B)$ can be defined in terms of bag constant, B which is the difference in the energy densities between perturbative (devoid of all particles and condensates) and non-perturbative QCD (includes chiral and gluon condensates). Also, the quark chemical potential, μ_q can be written as $\mu_q = \frac{\partial \epsilon}{\partial n_q} = p_F$ and the baryon chemical potential, $\mu_B = 3\mu_q$. Using these relations, the pressure and energy density (for $N_c = N_f = 3$) can be described as,

$$P(p_F) = ap_F^4 - B, \qquad \epsilon(p_F) = 3ap_F^4 + B \tag{4.34}$$

where $a = N_cN_f/4\pi^2$. The equation 4.34 gives the equation of state valid for non-interacting massless quarks. Such EOS results in the maximum mass and radius values (in terms of bag constant) as

$$M_{max} = 1.78\Big(\frac{155MeV}{B^{1/4}}\Big)^2 M_0 \tag{4.35}$$

$$R = 9.5\Big(\frac{155MeV}{B^{1/4}}\Big)^2 km \tag{4.36}$$

Strong interactions between quarks and gluons result in the breaking of the chiral symmetry of QCD by the chiral condensates which is basically the coupling of quark-antiquark pairs with different chirality (such as the formation of left-handed quark and right-handed anti-quark). Now in such condensed ground state, the excitation of quarks requires the

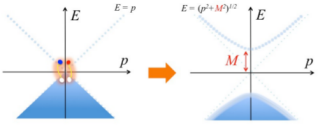

figure Chiral symmetry breaking via quark - antiquark pairing [BHK+17]

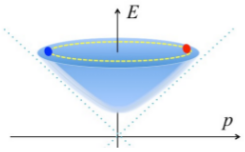

figure Quark-quark pairing leading to color superconductivity at high baryon density [BHK+17]

breaking of the pair, and hence the quark acquires an effective mass, M (due to the energy associated). The production of chiral condensates gives rise to changes in the structure of Dirac Sea which gives rise to non-perturbative QCD vacuum. This is depicted by fig. 4.5.1. Now the excited quark coming out of Dirac sea must be outside (in higher energy state) the fermi-sea in order to create a hole (or anti-quark) in Dirac sea. This creates a quark-sea, in which a *di-quark pairing* is possible where two quarks or two anti-quarks are paired just like electrons forming Cooper pairs in the superconductor (see fig. 4.5.1), this type of quark pairing gives rise to color superconductivity. Such phenomenon if present have a significant effect in the overall equation of state of neutron stars and hence should reflect a change in the macroscopic properties of it.

A widely used phenomenological model of interacting quarks in the dense matter is Nambu-Jona-Lasinio (NJL) model. The details of the model can be referred from [Kle92]. Next section discusses the construction of a generalized form of the EOS which follows the thermodynamic relations.

4.5.2 General Equation of State

While constructing a generalized equation of state, careful consideration should be on the stiffness of function and its implication on the overall structure. The most commonly used relation for the EOS is pressure, P as a function of the baryon chemical potential, μ_B. The pressure should be a monotonically increasing with respect to μ_B as the number density of baryons can then be defined by $n_B = \partial P/\partial \mu_B$, and it should have a positive slope with the chemical potential to be thermodynamically consistent and stable. Hence, apart from the continuity of pressure, for the stability of the system, we require

$$n_B = \partial P/\partial \mu_B > 0; \qquad \frac{\partial^2 P}{\partial \mu_B^2} = \frac{\partial n_B}{\partial \mu_B} > 0 \tag{4.37}$$

At a given value of chemical potential, a preferred phase will be the one with a higher value of pressure. Now, to construct the quark matter EOS, one can write the energy density in the form [BHK$^+$17],

$$\epsilon = A n_B^{4/3} + B - C n_B^{2/3} + D n_B^2 \tag{4.38}$$

In which the first term gives the kinetic energy of massless quarks, the second term is the density independent bag constant, the third term gives the contribution from pairing effects, and the fourth term is energy contribution from density-density vector repulsion (g_V) where $D \propto g_V$. Now, the baryon chemical potential and pressure can be obtained as

$$\mu_B = \frac{\partial \epsilon}{\partial n_B} = \frac{4}{3} A n_B^{1/3} - \frac{2}{3} C n_b^{-1/3} + 2 D n_B \tag{4.39}$$

$$P = n_B^2 \frac{\partial (\epsilon/n_B)}{\partial n_B} = \frac{1}{3} A n_B^{4/3} + \frac{1}{3} C n_B^{2/3} + D n_B^2 - B \tag{4.40}$$

4.5.3 Effect of g_V and H on the M-R relations

Now, the NJL model for dense quark matter contains a set of parameters, $g_V, H, K^{'}$ which can be partially fixed by matching to the QCD vacuum phenomenology. $K^{'}$ term (which couples the diquark condensate to quark condensate) is strongly correlated to the values of g_V and H. Therefore, here we will discuss the effects of variation of g_V and H on the EOS of the neutron star.

A higher value of H, i.e., the di-quark pairing interaction would mean an increase in the BCS pairing. This would result in stronger two-body correlations, and the quark matter is nearer to becoming confined. Therefore, the resulting pressure is shifted towards lower chemical potential. Also, increasing g_V which is the density vector repulsion would mean making it energetically costly for additional quarks to enter the system and have an effect of stiffening the equation of state. To see the effect on EOS more explicitly, we can assume the energy density to be,

$$\epsilon = \alpha n_B^{\gamma} \tag{4.41}$$

and the pressure and chemical potential then can be written as

$$P = \alpha(\gamma - 1) n_B^{\gamma}; \qquad \mu_B = \alpha \gamma n_B^{\gamma - 1} \tag{4.42}$$

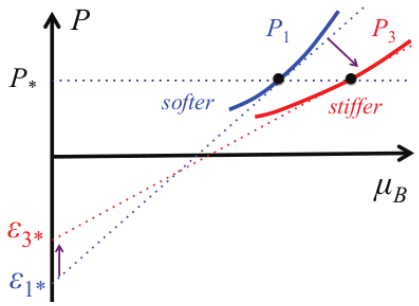

Figure 4.14: Variation of EOS from P_1 to P_3 as g_V is increased [BHT18]

To see the pressure variation with parameter α keeping energy density constant we can have,

$$\frac{\partial P}{\partial \alpha}\Big|_{\epsilon} = (\gamma - 1 - c_s^2) n_B^{\gamma} \tag{4.43}$$

where $c_s^2 = \partial P/\partial \epsilon\Big|_{\alpha}$ is the speed of sound.
Now, taking the repulsive interaction case, where the energy contribution is Dn_B^2 and $D \propto g_V$, we have $\gamma = 2$. Increasing the strength of g_V would result into higher value of pressure (see eq. 4.42) (with $c_s^2 < 1$ always) and hence a stiffer equation of state. This effect can be seen from the shift of EOS as the vector repulsion is increased (see fig. 4.14).

Similarly, increasing the pairing gap, Δ which gives a contribution in the parameter, C of the third term ($-Cn_B^{2/3}$) for energy density as $C \propto \Delta^2$ would give a γ value of $2/3$ with $\alpha = -C$. The resulting effect will result in a higher value of pressure as the negative value of C would counterbalance the negative value of $\gamma - 1$. Hence, the equation of state in result is stiffer.

The recent observation of massive binary pulsar resulting in a mass of around 2.01 requires the stiffening of EOS so that such masses can be taken into account. Thus, a larger value of g_V and H would surely help in finding a better fit to the equation of state. In the next section, a good fit to lower density EOS and interpolated EOS is discussed by using several higher values of the parameter g_V and H.

4.6 Interpolating methods

The EOS for hadronic matter (including nucleons) is well accepted for lower densities in a neutron star. But to evolve the structure of neutron star using TOV equations, it is required that the equation of state of matter for the densities from the surface to inner core is known. The EOS for hadronic matter which is acceptable for densities up to $2n_0$ cannot be simply extrapolated to higher densities as the role of strong interactions become more important, and one must use QCD at such level. Similarly, an EOS for pure quark matter (say given by NJL model) is well suited for higher densities (above $(4-7)n_0$) and cannot be extrapolated to be used at lower densities (below $4n_0$). This discrepancy in the validity of both the EOS's requires a correct prediction for the EOS in the intermediate region, i.e., for number densities between 2 to $4n_0$. Following method discuss a way to solve this discrepancy.

4.6.1 Hybrid Equation Of State

Hybrid construction of the equation of state considers a hadronic EOS for lower densities and a quark EOS at higher densities. The stable phase as discussed before is the one with a higher value of pressure at a given chemical potential. So we can restate, that the pressure of hadronic EOS is higher than the quark EOS at lower densities and it is higher for quark EOS at high densities. The point of intersection of both EOS at a specific pressure and chemical potential (p^*, μ_B^*) is the critical point of phase transition from hadronic matter to quark matter. While constructing a hybrid equation of state, it is required to make a Maxwell construction to equate the pressures and baryon chemical potentials between the quark-hadron phases. But, the main problem arises when one looks at the intersection point where ideally both the EOS must be valid, but in actuality, the hadron EOS is uncertain due to the involvement of many-body and hyperon forces and the quark EOS is uncertain due to the confinement effects.

Another important point to take into account is that both EOS must actually intersect and cannot take non-intersecting EOS's as it would violate the low and high-density EOS validity (as the pressure would remain higher for one of them), see fig. 4.15. Also, a first order phase transition occurs at $\mu_{H\to Q}$ which should be consistent thermodynamically.

Even though such approach provides many constraints on the EOS, it has a serious draw-

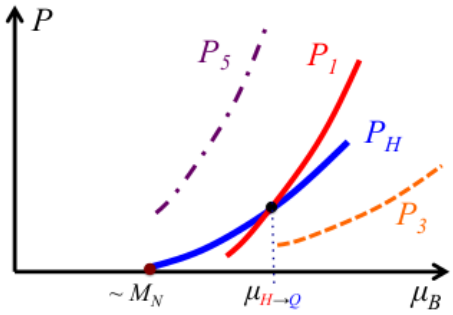

Figure 4.15: Stiff EOS P_5 and P_3 are not included as they do not intersect [BHT18]

back as it assumes that at the point of intersection both of the EOS should be valid. Hence, if the value of the chemical potential at which the intersection occurs, is higher there exist serious doubts on the validity of hadronic EOS and if intersection occurs at a lower value of μ_B it develops inconsistency in quark EOS. A more consistent approach is the unified construction of EOS as discussed below.

4.6.2 Unified Equation Of State

In this approach, the hadronic and quark EOS are used only in the region of their validity and for the intermediate region an interpolated equation of state should be developed in a consistent method. To use appropriate EOS in their validity region, it is important to make the cutoff number densities for both higher and lower density regimes. Hence, we can consider hadronic EOS to be valid only below number density, n_{BL} and quark EOS (NJL) to be valid for densities higher than say, n_{BU}. In the region between n_{BL} and n_{BU}, none of the developed models is applicable, and one has to develop a thermodynamically consistent EOS. In developing such EOS, one should take into account that the pressure of interpolated EOS at μ_{BL} and at μ_{BU} must match with the hadronic and quark EOS values at these points. Also, the thermodynamic stability condition ($\partial n_B/\partial\mu_B = \partial^2 P/\partial\mu_B^2 > 0$) must be satisfied along with the causality constraint of $c_s^2 = \partial P/\partial\epsilon < c^2$. An advantage of this method is that there is no region where a direct competition of two EOS (hadron and quark) has been made, and one can safely consider several stiff quark EOS to match with the recent observations.

To construct the interpolating EOS, one can assume the pressure in the intermediate regime

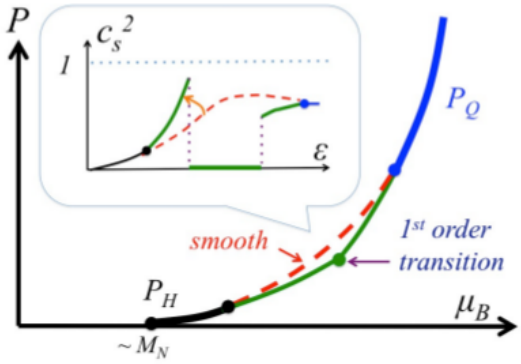

Figure 4.16: Plot showing higher chances of violating causality relation if first order transition occurs [BHT18]

as a polynomial expansion given as

$$P(\mu_B) = \sum_{m=0}^{N} C_m \mu_B^m \tag{4.44}$$

where C_m can be found from the matching conditions. Further constraints to match the EOS with boundary can be written as,

$$P(\mu_{BL}) = P_H(\mu_{BL}), \frac{\partial P}{\partial \mu_B}\Big|_{\mu BL} = \frac{\partial P_H}{\partial \mu_B}\Big|_{\mu BL}, ... \tag{4.45}$$

$$P(\mu_{BU}) = P_H(\mu_{BU}), \frac{\partial P}{\partial \mu_B}\Big|_{\mu BU} = \frac{\partial P_Q}{\partial \mu_B}\Big|_{\mu BU}, ... \tag{4.46}$$

To have continuous pressure, number density and susceptibility ($\partial n_B/\partial \mu_B$) one should match upto second derivative. Another point to take into account is the appearance of first order phase transition (which appears as a kink in the EOS) in the intermediate region. Even though such transition is not completely ruled out of the construction, the possibility of its existence is strongly constrained due to the boundary matching conditions as well as the speed of sound constraint (See fig. 4.16). Thus, at low temperatures there should not be a strong first order chiral restoration transition in QCD.

In the 2018 paper by Gordon Baym, Tetsuo Hatsuda et al.[BHT18], varying values of g_V and H are considered such as to fit with the hadronic EOS and quark EOS along with no inflection point and kink so that all physical inconsistencies can be avoided. This is done in a way that first g_V is changed as a parameter, keeping $H = 0$ (see fig. 4.17), then once an appropriate value (0.8) of g_V is fixed, the value of H is varied (see fig. 4.18) to fix the final

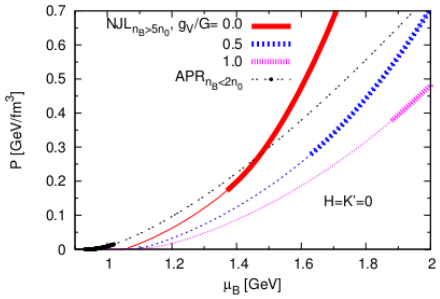

Figure 4.17: Varying values of g_V are tested, keeping $H = 0$ and the comparison with the extrapolated APR EOS is shown [BHT18]

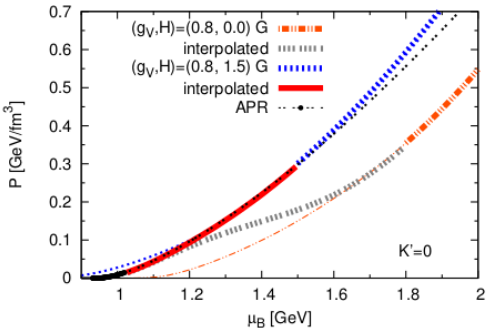

Figure 4.18: Varying values of H are plotted keeping g_V fixed at 0.8 and the comparison with the extrapolated APR EOS is shown [BHT18]

parameter point of (g_V, H). The interpolated EOS found and the fixed value of g_V and H is dependent on the EOS used in the lower density regimes.

In order to develop a complete set of equation of state with the same form and tuning it such that it satisfies the needs of each domain, a method of parameterization has been presented in the review by Baym et al. [BHT18]. The parametric form of energy density ϵ in terms of $\xi = n_B/n_0$ can be written as,

$$\epsilon(\xi) = a\xi + d_0 + d_1\xi ln\xi + \sum_{\nu=2}^{\nu_{max}} d_\nu \xi^{l_\nu} \tag{4.47}$$

where a, d_n's, ν_{max} and l_ν are the fitting parameters which can be found depending on the region. Using eq. 4.47, one can find chemical potential and pressure as,

$$\mu_B(\xi) = \frac{1}{n_0}\left[a + d_1(1 + ln\xi) + \sum_{\nu=2}^{\nu_{max}} l_\nu d_\nu \xi^{l_\nu - 1}\right] \tag{4.48}$$

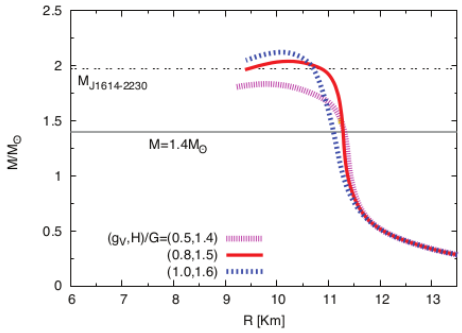

Figure 4.19: Total mass and radius values for a stable neutron star with varying quark EOS parameters [BHT18]

$$P(\xi) = -d_0 + d_1\xi + \sum_{\nu=2}^{\nu_{max}} (l_\nu - 1) d_\nu \xi^{l_\nu} \tag{4.49}$$

The pressure at each point is used to determine the d_i's in the equations above. The fitting parameters are found by using the already known EOS for hadron and quark regions and the interpolated EOS is then adjusted accordingly.

In the paper by Baym [BHT18], Togashi EOS [TNT$^+$17] for the crust region ($< n_B < 0.26n_0$), APR EOS ([APR98]) in the liquid region ($0.26n_0 < n_B < 2n_0$), interpolated (QHC'18 crossover) EOS in the intermediate region ($2n_0 < n_B < 5n_0$) and Quark EOS (NJL model) in the high density region ($n_0 < n_B < 10n_0$) to fit the paremetric form have been used. The total mass versus total radius relationship for a stable neutron star (See fig. 4.19) is obtained using it. The maximum mass is found to be slightly different for varying parameter values but all the final EOS's developed were stiff and hence higher values of maximum mass are obtained which satisfies with the recent observation of $2.01M_0$.

4.7 Developing a new EOS

In an attempt to develop an equation of state which achieves the maximum mass limit of the neutron star, different equation of states can be combined according to their validity, and the TOV equations can then be evolved. This section discusses the combination of such realistic EOS's and their results. The model by BPS (as discussed in section 4.3) can be used to perfectly describe the crust of neutron stars and is used for the mass densities ranging from $10^{26}\ kgkm^{-1}s^{-2}$ to $10^{31}\ kgkm^{-1}s^{-2}$.

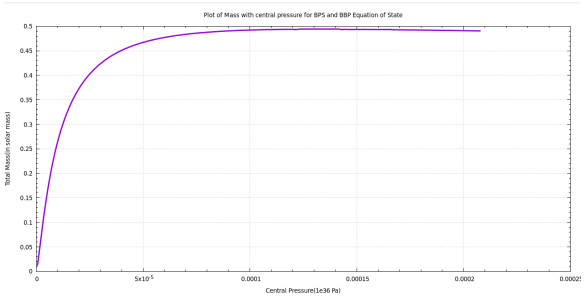

Figure 4.20: Total mass and central pressure values including BPS [Bay71a] and BBP [Bay71b] models for equation of state

Another well-established model for the mass densities above neutron drip (4.3×10^{11} gcm^{-3}) where neutrons start to drip out of the nuclei is given by Baym, Bethe, and Pethick (BBP [Bay71b]). This model considers the liquid drop model in order to take into account the effect of neutron-rich nuclei immersed in a sea of free neutrons. The three important aspects considered in this paper are the effects i) that the bulk nuclear matter in the nuclei and the pure neutron gas outside nuclei become similar to each other as the density is increased, ii) of the decrease in surface energy due to the presence of free neutron gas ,and iii) of Coulombic interactions between nuclei to develop a lattice.

Now, considering BPS model for the crust before neutron drip and BBP model above neutron drip, TOV equations have been solved in the code and plot of total mass variation with central pressures is shown in fig. 4.20. The plot of neutron stars with total mass and radius consistent with the EOS have been developed (see fig. 4.21). The maximum mass value is about $0.495M_0$ which suggests that a different state of matter at extremely dense regimes is required to reach a correct prediction.

To achieve a stiff equation of state so that the upper limit of neutron star masses is attained, we use Akmal-Pandharipande-Ravenhall (APR) equation of state [APR98]. The variations of the total mass with central pressures can be seen in fig. 4.22. Further, the total mass with radii plot (see fig. 4.23) shows the maximum mass limit to reach upto $3M_0$ which allows the observed value of $2.01M_0$.

A recent review article by Gordon Baym, Tetsuo Hatsuda, et al. [BHK$^+$17], develops the equation of state for the hadronic and quark part and fits the parameters considering a generalized form for the equations given by eqs. 4.47,4.48, 4.49. The EOS developed by

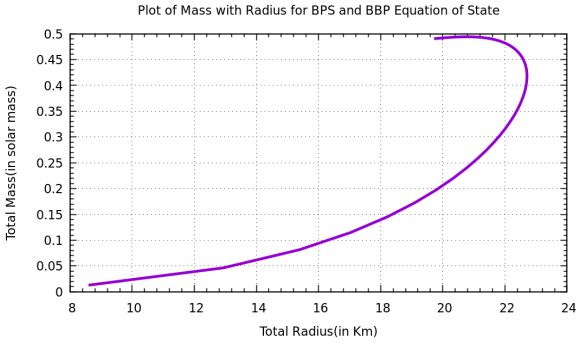

Figure 4.21: Total mass and total radius values including BPS [Bay71a] and BBP [Bay71b] models for equation of state

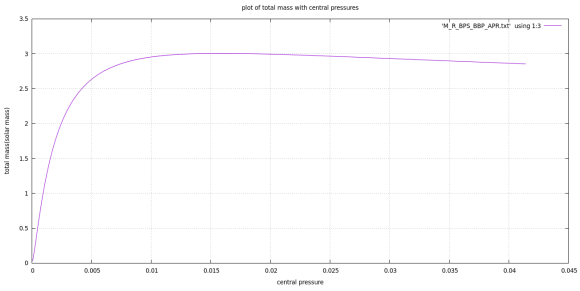

Figure 4.22: Total mass and central pressure values including BPS [Bay71a], BBP [Bay71b] and APR [APR98] models for equation of state

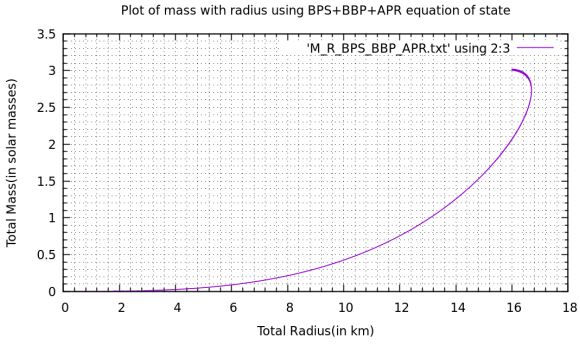

Figure 4.23: Total mass and total radius values including BPS [Bay71a], BBP [Bay71b] and APR [APR98] models for equation of state

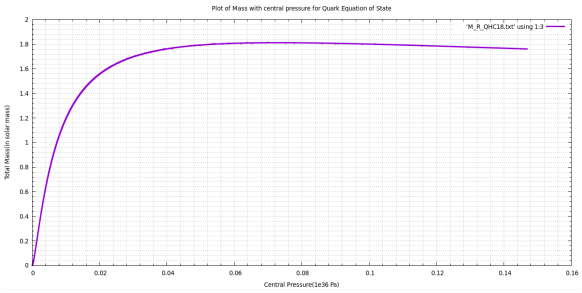

Figure 4.24: Total mass and central pressure values including quark (NJL) model as equation of state [BHK$^+$17]

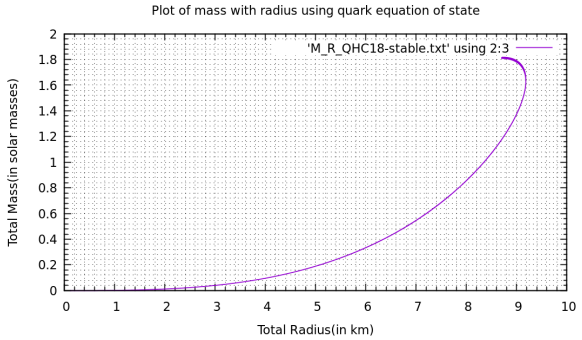

Figure 4.25: Total mass and total radius values including quark (NJL) model as equation of state [BHK$^+$17]

this mechanism at higher densities (called QHC'18) have been used in the quark regime. The plot for total masses and central pressures is given in fig. 4.24 and the plot for mass, radius variation is shown in fig. 4.25.

Due to immense mass densities inside the core of massive neutron stars, the possibility of quark matter has to exist as depicted by the temperature-chemical potential curve in fig. 1.1. As explained in chapter 1 of this thesis, the existence of quark matter in 'De-confined' state have a reduced volume as compared to the volume of the pure hadronic matter. This in effect should have a significant implication in the total radius of the neutron star, and hence the radius of a hybrid star with a quark core must be smaller as compared to a normal neutron star with no hadron-quark phase transition. One can also predict this by looking at the stable mass-radius plots considering the equation of states for pure hadronic matter (BPS+BBP+APR) and pure quark matter (QHC'18) (see fig. 4.26).

The radii of the hybrid star is found with varying ratios of quark and hadronic matter for a constant total mass (here $1.6M_0$). To implement this, C++ code is developed which invokes

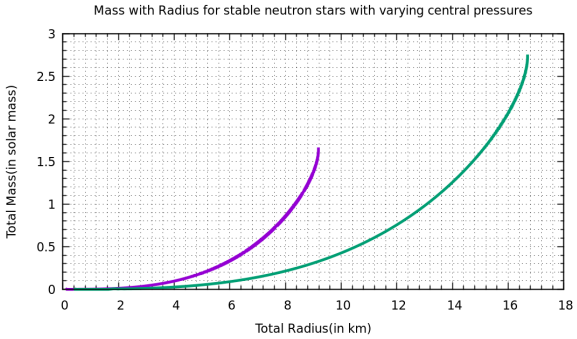

Figure 4.26: Total mass and total radius values with quark model (purple curve) and hadronic model (blue curve) as the equation of state

the equation of states by BPS, BBP and APR models (developed in a functional form by interpolating) in lower density regimes and QHC'18 [BHK$^+$17] at high densities. First, the percentage of total mass which is to be considered quark matter and the hadronic matter is decided (starting from 0% to 100%) and the radius of quark matter is calculated (considering QHC'18 with g_V=0.7 and H=1.4). The remaining mass must be hadronic, and the TOV equations are then solved backward to calculate the radii of the hadronic part when the mass inside matches with that of the quark matter inside. The total radius then calculated from various percentages of the hadronic matter is plotted (see fig. 4.27). This study gives a direct implication that the total radius of the star must decrease with the increase in the amount of quark matter at the core. The values of total radius for each of the quark matter percentages and the percentage change in the radius are calculated. The maximum change in the radius is calculated to be about 39.25%. When 50% of the quark matter is present, and other 50% is the hadronic matter, the total radius of the neutron star reduces to about 75% of its radius value when only pure hadrons were present inside it.

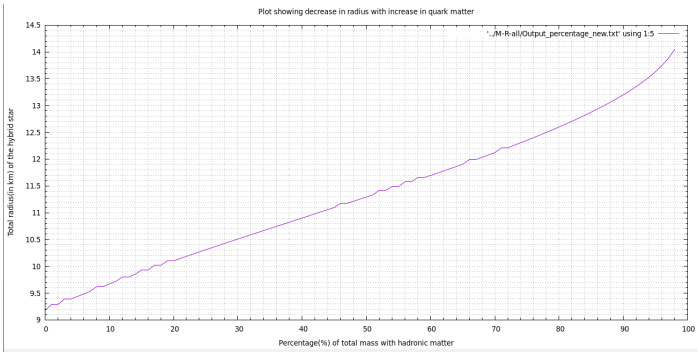

Figure 4.27: With increasing percentage of hadronic matter the total radius of the star is increased for a constant total mass

Further, to determine the critical radius at which the quark-hadron phase transition occurs, the TOV equations were solved backward for different critical radii, and the EOS for quark and hadronic parts were used accordingly. The values of total mass and radius for which reasonable values of mass and pressure at the core were found, was taken to be the correct prediction. The value of total mass with a quark core inside comes out to be $2.1\ M_0$, and the corresponding radius is 16 km. The critical radius at which the phase transition should have occurred ranges from 2.25 km to 2.44 km.

Bibliography

[APR98] A. Akmal, V. R. Pandharipande, and D. G. Ravenhall, *Equation of state of nucleon matter and neutron star structure*, Phys. Rev. C **58** (1998), 1804–1828.

[Bay71a] Christopher; Sutherland Peter Baym, Gordon; Pethick, *The ground state of matter at high densities: Equation of state and stellar models*, Astrophysical Journal, vol. 170, p.299 (ApJ Homepage) (Dec, 1971).

[Bay71b] Hans A.; Pethick Christopher J Baym, Gordon; Bethe, *Neutron star matter*, Nuclear Physics A **175** (1971), 0375–9474.

[BBP71] G. Baym, H. A. Bethe, and C. J. Pethick, *Neutron star matter*, Nuclear Physics A **175** (1971), 225–271.

[BHK+17] G. Baym, T. Hatsuda, T. Kojo, P. D. Powell, Y. Song, and T. Takatsuka, *From hadrons to quarks in neutron stars: a review*, ArXiv e-prints (2017).

[BHT18] Gordon Baym, Tetsuo Hatsuda, and Tatsuyuki Takatsuka, *From hadrons to quarks in neutron stars: a review*, Reports on Progress in Physics (2018).

[CW74] S. A. Chin and J. D. Walecka, *An equation of state for nuclear and higher-density matter based on relativistic mean-field theory*, Physics Letters B 52.1 (1974), 25–28.

[DGRW83] C. J. Pethick D. G. Ravenhall and J. R. Wilson, *Structure of matter below nuclear saturation density*, Phys. Rev. Lett. 50, 2066 (1983).

[ea13] J. Antoniadis et al., *A massive pulsar in a compact relativistic binary*, Science 340, 1233232 **69** (2013).

[GCR12] S. Gandolfi, J. Carlson, and Sanjay Reddy, *Maximum mass and radius of neutron stars, and the nuclear symmetry energy*, Phys. Rev. C **85** (2012), 032801.

[Gle97] Norman K. Glendenning, *Compact stars nuclear physics, particle physics, and general relativity*, Astronomy and Astrophysics Library (1997).

[HB64] Proc. R. Soc. H. Bondi, London (1964), no. A282, 303.

[Kle92] S. P. Klevansky, *The Nambu-Jona-Lasinio model of quantum chromodynamics*, Rev. Mod. Phys. **64** (1992), 649–708.

[LP04] J.M. Lattimer and M. Prakash, *The physics of neutron stars*, 1–4.

[LP15] _____, *The equation of state of hot, dense matter and neutron stars*.

[LP16] J.M. Lattimer and M. Prakash, *The equation of state of hot, dense matter and neutron stars*, 127–164, Provided by the SAO/NASA Astrophysics Data System.

[NYT14] S. Benić D. Blaschke T. Maruyama N. Yasutake, R. Łastowiecki and T. Tatsumi, *Finite-size effects at the hadron-quark transition and heavy hybrid stars*, Phys. Rev. C 89, 065803 (2014).

[Pan71] V. R. Pandharipande, *Hyperonic matter*, Nuclear Physics A **178** (1971), 123–144.

[Piz] Pierre M. Pizzochero, *Exploring fundamental physics with neutron stars*.

[TNT+17] H. Togashi, K. Nakazato, Y. Takehara, S. Yamamuro, H. Suzuki, and M. Takano, *Nuclear equation of state for core-collapse supernova simulations with realistic nuclear forces*, Nuclear Physics A **961** (2017), 78–105, Provided by the SAO/NASA Astrophysics Data System.